ISSN 0030-6096

OSAKA CITY MEDICAL JOURNAL

Vol. 72
No. 1

2026

PUBLISHED BY
OSAKA CITY MEDICAL ASSOCIATION
OSAKA JAPAN

Osaka City Medical Journal
Vol. 72, No. 1, June 2026

CONTENTS

Osaka City Med. J. Vol. 72, 1-9, 2026

Effects of Rehabilitation on the Post-acute Phase of Patients with COVID-19 Pneumonia in a Convalescence Ward

Mitsuhiko Ikebuchi[1)], Yoichi Ohta[1)], Yukihide Minoda[1)], Hidetomi Terai[1)], Hiroaki Nakamura[2)], Akiko Toki[4)], and Tamotsu Nakatsuchi[1,3)]

Department of Orthopedic Surgery[1)], Graduate School of Medicine, Osaka Metropolitan University; Osaka Metropolitan University Hospital[2)]; Tsuji-geka Rehabilitation Hospital[3)]; and Departments of Rehabilitation Medicine[4)], Osaka General Medical Center

Abstract

Background

This study aimed to investigate discharge destinations and the factors influencing them for patients with post-acute phase COVID-19 pneumonia in the convalescence ward.

Methods

This study included patients with post-acute phase COVID-19 pneumonia admitted to the convalescence ward from July 2020 to May 2022. Patients were categorized by discharge living environment changes: unchanged, improved, or declined from onset. A comparative analysis was conducted for 37 items, including age, sex, comorbidities, and Functional Independence Measure (FIM) scores at admission and discharge.

Results

This study included 57 patients (32 men, 25 women) with a mean age of 75.8±9.6 years (range: 51-94). At the onset of COVID-19 pneumonia, the living environment was home for 39 patients, care home for 14, and hospital for 4. Discharge destinations included home for 35 patients, care home for 18, and hospital for 4. Among these, eight patients experienced a decline in the living environment. Factors that hindered the recovery of the living environment were a history of heart disease and the Motor FIM score at admission.

Conclusions

This study identified low activity during admission to the convalescence ward as a factor inhibiting the improvement of the living environment after discharge, suggesting the usefulness of rehabilitation during the acute phase.

Key Words: Functional recovery; COVID-19 pneumonia; Post-acute phase rehabilitation

Received January 16, 2025; accepted June 10, 2025.

Correspondence to: Tamotsu Nakatsuchi, PhD.
Department of Orthopedic Surgery, Graduate School of Medicine, Osaka Metropolitan University, 1-4-3 Asahimachi, Abeno-ku, Osaka 545-8585, Japan
Tel: +81-6-6645-3851; Fax: +81-6-6646-6260
E-mail: nakatsuchi@kankikai.com

Introduction

Since its initial report in 2020, coronavirus disease (COVID-19) pneumonia has rapidly spread worldwide, resulting in a significant number of infections. The presence of post-recovery sequelae and impaired activities of daily living (ADL) is well-documented, prompting discussions about the necessity of rehabilitation after symptom stabilization[1-5].

In Japan, a system for post-acute rehabilitation is in place, occurring after the specialized treatment of acute illnesses or injuries, once the condition of the patient has stabilized. This system aims to facilitate functional recovery, improve diminished abilities and activities, and promote the home return. Specialized beds, the convalescence ward, are provided for this purpose, with a specified period during which improvement is expected, assessed using the Functional Independence Measure (FIM). This rehabilitation framework has been applied to patients with COVID-19 pneumonia, particularly from Japan's second wave of the pandemic, playing a role in the rehabilitation of patients in the post-acute phase.

The convalescence ward, an affiliated facility of our institution, has a for admitting patients with post-acute phase COVID-19 pneumonia since the second wave. This study aimed to investigate the discharge destinations and factors influencing them for patients with post-acute phase COVID-19 pneumonia in the convalescence ward.

Methods

Study design and patient population

The spread of COVID-19 in Japan was classified as a Class Ⅱ infectious disease. In the Osaka Prefecture, where Tsuji-Geka Rehabilitation Hospital (TGRH) is located, patients diagnosed with the need for hospitalization were transported to acute hospitals with negative-pressure rooms, coordinated by the Public Health Center. At these hospitals, treatment was administered under confinement. Patients were released from confinement when they met the release criteria at least 10 days after the infection was confirmed. Upon symptom stabilization, they were transferred to post-acute hospitals for continued care until discharge. Patients who presented with difficulty in returning home were transferred to the convalescence ward.

This study included patients with COVID-19 pneumonia admitted to the convalescence ward of TGRH from July 2020 to May 2022. The study period covered the waves of the COVID-19 pandemic in Japan, spanning from the second to the sixth wave. TGRH admits patients with post-acute phase COVID-19 pneumonia who are assessed as having difficulty in returning home and whose FIM score at the time of the previous hospital discharge was 115 points or below. Those with an unknown history of steroid use were excluded.

Written informed consent could not be obtained, given the constraints imposed by the retrospective design. Participants could withdraw from this study at any time using an opt-out procedure. This study was reviewed and approved by the ethics committee of TGRH (No. 55).

Rehabilitation program

In the convalescence ward, the focus is not on treating the disease but on rehabilitation. Thus, the primary objectives are functional recovery, improvement of diminished abilities and activities, and the facilitation of the home return. Rehabilitation, lasting up to 3 h daily, is provided during days 60 to 180 of hospitalization, depending on the condition. The facility also addresses post-discharge environmental adjustments and coordinates with community resources, aiming for maximal

functional recovery and home environment adjustment to facilitate the home return. A maximum hospitalization period of 90 days is established with the disease name "Disuse Syndrome", designated by medical insurance.

In the convalescence ward of TGRH, rehabilitation for patients with COVID-19 pneumonia follows indications tailored for Disuse Syndrome. Physical therapists conduct respiratory training, muscle-strengthening exercises, and endurance training, while occupational therapists provide ADL guidance. Additional speech therapy, including vocalization exercises, is incorporated for patients who have undergone procedures such as tracheostomy. Specifically, the process begins with respiratory training by a physical therapist to secure seated time. Once stability in the seated position is achieved, rehabilitation progresses to walking and ADL training. Upon achieving independent ADL within the ward, discharge arrangements are made, leading to the eventual discharge of the patient. The initiation of discharge arrangements typically occurs between days 30 and 60 into hospitalization, as the maximum hospitalization period is 90 days.

Data collection

The survey items included the phase of the COVID-19 pandemic (second to sixth wave); age, sex, height, and weight; body mass index (BMI) and the presence of obesity or low body weight; living environment at onset; discharge destinations; duration from onset to admission to the convalescence ward and length of hospitalization at the convalescence ward; intubation in the acute phase, use of oxygen, tracheostomy, and presence of pulmonary edema or atelectasis at admission; use of steroids and anti-COVID medications in previous medical treatments; introduction of hot oxygen therapy (HOT) at discharge; presence of comorbidities such as hypertension, diabetes mellitus, hyperlipidemia, renal diseases, respiratory diseases, heart diseases, cerebrovascular disorders, musculoskeletal disorders (including trauma), Parkinson's disease, and dementia; number of comorbidities; and Motor FIM and Cognitive FIM scores at admission and discharge and their FIM Effectiveness. Regarding obesity and low body weight, the criteria of the Japan Society for the Study of Obesity were used, which define obesity as a BMI of 25.0 or higher and low body weight as a BMI of 18.5 or lower.

Outcome measurement

The cases were categorized based on changes in the living environment from onset to discharge. Group I comprised cases where the living environment remained the unchanged or improved at discharge compared to onset, such as from care home at onset to care home at discharge. Group D included cases whose living environment at discharge declined from onset, such as home to hospital. A comparative analysis was conducted for each survey item.

Statistical analysis

Fisher's exact test and Mann-Whitney U-test were performed for the two-group comparison, and a p-value <0.05 was considered statistically significant. Effect size was calculated using Odds ratio for Fisher's exact test and R-value (R=Z/square root N) for Mann-Whitney U-test. Factor analysis was not performed because there were not enough cases to obtain valid statistical results.

The statistical calculation software R for Mac OS X Cocoa GUI version 3.6.2 (R Core Team) was used for analysis[6].

Results

Characteristics of the patients

The study included 57 of 63 patients (32 men, 25 women) with COVID-19 pneumonia admitted to

the convalescence ward of TGRH from July 2020 to May 2022. Six cases were excluded owing to incomplete data. Patients at admission ranged from 51 to 94 years, with a mean age of 75.8±9.6 years. Further details are presented in Table 1.

A total of 17 cases required intubation in the acute phase, with two of them undergoing tracheostomy and requiring oxygen administration. However, both cases achieved tracheostomy closure and oxygen withdrawal during hospitalization in the convalescence ward.

Among the discharged cases, two required HOT, one of which was required intubation in the acute phase. They neither had a history of lung disease nor underwent tracheostomy, but both were admitted with oxygen supplementation owing to atelectasis observed on the initial computed tomography scan at admission. Despite extended hospitalizations of 126 and 88 days, both cases were discharged to their homes.

As for comorbidities at the time of admission, factors contributing to the severity for COVID-19 pneumonia, such as hypertension, diabetes mellitus, hyperlipidemia, renal diseases, and respiratory diseases, were observed in 35, 25, 18, 1, and 6 cases, respectively. Other complications affecting ADL included heart diseases, cerebrovascular disorders, musculoskeletal disorders, with 9, 11, 14, 5, and 5 cases, respectively.

At the onset of COVID-19 pneumonia, the living environment was home for 39 cases, care home for 14 cases, and hospital for 4 cases. Among those in a home setting at onset, two cases with a history of stroke were confirmed as requiring long-term care. The FIM score at admission was 60.7± 22.1 (range: 19-106); Motor FIM: 35.4±16.9 (13-71), Cognitive FIM: 25.3±8.2 (6-35). Discharge destinations included home for 35 cases, care home for 18 cases, and hospital for 4 cases. Among these, 8 cases experienced a decline in the living environment. Specifically, the living environment of four cases changed from home at onset to care home at discharge, that of one case changed from care home at onset to hospital at discharge, and those of three cases changed from home at onset to hospital at discharge. Four cases exhibited improvements in their living environments, including three cases changing from hospital at onset to home at discharge and one case from hospital at onset to care home at discharge. For 45 cases, the living environment remained unchanged between onset and discharge.

The FIM score at discharge was 92.9±33.0 (range: 24-126), with Motor FIM at 65.9±25.7 (range: 13-91) and Cognitive FIM at 27.1±8.6 (range: 10-35). The Motor and Cognitive FIM Effectiveness were 30.4±20.7 (range: −5-77) and 1.8±2.5 (range: 0-12), respectively. These scores exhibited significant improvement compared to those observed at admission (paired t-test $p<0.05$).

Subgroup analysis

Further results are presented in Table 1. Group I consisted of 49 cases (28 men, 21 women), and Group D comprised 8 cases (4 men, 4 women). There were no statistically significant differences between the two groups in age, sex, height, weight, BMI, and the phase of the COVID-19 pandemic. For other survey items, including presence of obesity or low body weight, living environment at onset, duration from onset to admission to the convalescence ward and length of hospitalization at the convalescence ward, intubation in the acute phase, use of oxygen, tracheostomy, presence of pulmonary edema or atelectasis at admission, use of steroids and anti-COVID medications in previous medical treatments, and introduction of HOT at discharge, there were no statistically significant differences between the two groups.

In terms of comorbidities, statistically significant differences were observed only in heart diseases

Table 1.

	Total (n=57)	Group I (n=49)	Group D (n=8)	P-value (Group I vs Group D)	Effect Size
Wave					
2nd	2	2	0		
3rd	1	1	0		
4th	29	25	4	N.S	
5th	4	4	0		
6th	21	17	4		
Age (years)	75.8±9.6 (51-94)	75.5±9.7 (51-94)	77.9±9.0 (61-90)	N.S	
Male	32	28	4	N.S	
Height (cm)	159.5±11.0 (138-181)	159.9±11.0 (138-181)	157.1±11.5 (138-173)	N.S	
Weight (kg)	54.1±14.3 (28.3-97.8)	54.5±14.3 (28.3-97.8)	51.7±15.0 (31.8-78.1)	N.S	
BMI	21.2±4.8 (11.7-32.0)	21.2±4.9 (11.7-32.0)	20.7±4.4 (16.7-27.3)	N.S	
Obesity	13	11	2	N.S	
Low Body Weight	17	13	4	N.S	
Living Environment at Onset					
Home	39	32	7		
Care House	14	13	1	N.S	
Hospital	4	4	0		
Duration from Onset to Admission (days)	31.8±24.3 (9-136)	30.8±20.9 (9-130)	37.8±41.0 (12-136)	N.S	
Length of Hospitalization (days)	56.3±30.1 (7-126)	58.2±29.9 (7-126)	45.1±30.8 (10-95)	N.S	
Intubation in the Acute Phase	17	15	2	N.S	
Use of Oxygen	23	19	4	N.S	
Tracheostomy	2	2	0	N.S	
Pulmonary Edema	26	22	4	N.S	
Atelectasis	41	34	7	N.S	
Use of Steroids and Anti-COVID medications	44	37	7	N.S	
HOT at Discharge	2	2	0	N.S	
Comorbidities:					
Hypertension	35	29	6	N.S	
Diabetes Mellitus	25	19	6	N.S	
Hyperlipidemia	18	14	4	N.S	
Renal Diseases	1	1	0	N.S	
Respiratory Disease	6	6	0	N.S	
Heart Disease	9	5	4	p<0.05	Odds ratio: 8.80
Cerebrovascular Disorder	11	10	1	N.S	
Musculoskeletal Disorders	14	13	1	N.S	
Parkinson Disease	5	5	0	N.S	
Dementia	5	5	0	N.S	
Numbers of Comorbidities					
Four Comorbidities	3	1	2		
Three Comorbidities	15	12	3		
Two Comorbidities	15	14	1	N.S	
One Comorbidities	18	16	2		
No Comorbidities	6	6	0		
At Admission					
Motor FIM	35.4±16.9 (13-71)	38.3±16.3 (13-71)	17.6±5.4 (13-27)	p<0.05	R=0.5
Cognitive FIM	25.3±8.2 (6-35)	25.9±8.2 (6-35)	21.3±7.8 (10-33)	N.S	
At Discharge					
Motor FIM	65.9±25.7 (13-91)	70.8±22.2 (14-91)	35.6±26.5 (13-88)	p<0.05	R=0.4
Cognitive FIM	27.1±8.6 (10-35)	27.9±8.4 (10-35)	22.0±8.5 (10-33)	p<0.05	R=0.3
Motor FIM Effectiveness	30.4±20.7 (−5-77)	32.5±19.5 (1-77)	18.0±24.5 (−5-65)	N.S	
Cognitive FIM Effectiveness	1.8±2.5 (0-12)	2.0±2.6 (0-12)	0.8±1.4 (0-4)	N.S	

Abbreviations: BMI, Body mass index; HOT, Home oxygen therapy; and FIM, the Functional Independence Measure.
Formula: Effective Size R=Z/square root N.

(Group I: 5 cases, 10.2%, Group D: 4 cases, 50%), suggesting a higher incidence of heart diseases in Group D (Fisher test: $p<0.05$, Odds ratio: 8.80). However, there were no statistically significant differences between the two groups in the number of complications.

In terms of the FIM score, the Motor FIM scores were significantly lower in Group D at both admission and discharge, while Cognitive FIM scores at discharge were significantly lower in Group D. Regarding effect size R, the Motor FIM score at admission showed a large effect ($R=0.5$), the Motor FIM score at discharge showed a moderate effect ($R=0.4$), and the Cognitive FIM score at discharge also showed a moderate effect ($R=0.3$). However, there were no statistically significant differences between the two groups regarding Cognitive FIM at admission, Motor and Cognitive FIM Effectiveness scores.

Discussion

COVID-19 pneumonia is known for its strong infectivity and can sometimes worsen, leading to death. According to reports based on the COVID-19 Registry Japan (COVIREGI-JP), a registry for COVID-19 pneumonia in Japan, Risk factors for severity include male sex, older age, obesity, diabetes mellitus, and chronic obstructive pulmonary disease[7]. The data also indicate a high mortality rate in patients requiring artificial ventilation, with an increased risk of death in older individuals. Male sex is highlighted as a significant risk factor for survival or mortality, and the coexistence of connective tissue diseases, kidney disorders, and dialysis treatment are also reported as significant risk factors[8,9]. However, this study demonstrated that risk factors for severity and mortality for COVID-19 pneumonia did not impact the recovery of the living environment. The only complication that influenced the recovery of the living environment was the presence or absence of heart diseases. Other complications did not emerge as a contributing factor, and the presence of pulmonary edema or atelectasis did not affect the recovery either. These results suggest that with sufficient treatment during the acute phase, COVID-19 pneumonia may not have a lasting impact on the recovery of the living environment.

The standard treatment for COVID-19 pneumonia includes antiviral drugs, neutralizing antibodies, and steroid administration. Concerns have been raised about the potential impact of treatment duration differences in the acute phase due to the presence or absence of medication, as well as the effects of medication-related side effects such as steroid myopathy. However, this study suggests that the presence or absence of medication does not impact the recovery of the living environment.

In patients with COVID-19 pneumonia, the decline in ADL after symptom remission poses a concern. Several reports have highlighted the importance of rehabilitation during the post-acute phase, once the infection risk has significantly decreased. These studies indicated that patients with COVID-19 pneumonia often experience sustained respiratory function impairment and that respiratory rehabilitation during the post-acute phase is effective in preventing respiratory, walking, and cognitive function decline[1-5]. In this study, Motor FIM and Cognitive FIM scores improved by 30.4 ± 20.7 (range: -5-77) and 1.8 ± 2.5 (range: 0-12), respectively. This finding is consistent with previous studies and suggests that rehabilitation during the post-acute phase may effectively improve ADL and prevent cognitive function decline. Furthermore, some reports suggest the persistence of decreased lung function in the chronic phase[10-12]. In this study, cases that required the introduction of HOT were discharged to their homes. Despite the potential decline in lung function, the results

suggest that with sufficient time and appropriate interventions, maintaining ADL is feasible.

In this study, factors that hindered improvements in the living environment were a history of heart disease and the Motor FIM score at admission. There was no significant difference in the FIM Effectiveness between Group I and Group D. Additionally, no statistical significance was observed intubation in the acute phase or days from onset to admission. These findings suggest that substantial improvement in Motor FIM at admission is necessary for improvements in living conditions. The Stanford Hall consensus statement recommends a holistic approach for COVID-19 pneumonia cases requiring rehabilitation, as they may exhibit post-intensive care syndrome similar to ICU patients[13]. Ceravolo et al, based on a systematic search conducted until March 31, 2020, suggested the necessity of allowing early rehabilitation for hospitalized patients with COVID-19 pneumonia[14]. The authors reported improved activity in severe COVID-19 pneumonia cases through early rehabilitation during the hyperacute phase[15]. The findings suggest that early rehabilitation, initiated from the hyperacute phase, may be effective for the home return in COVID-19 pneumonia cases.

Regarding the history of heart disease as a factor hindering improvements in the living environment, the convalescence ward of TGRH cannot admit patients with a history of heart disease requiring exercise restrictions. Therefore, the exercise load should remain consistent regardless of whether a patient has a history of heart disease. However, when we categorized the cases based on the presence or absence of a history of heart disease and compared them, we found that those with a history of heart disease (9/57 cases) had a Motor FIM score of 25.7±12.6 (13-45) at admission, a Motor FIM score of 46.8±26.6 (13-81) at discharge, and a Motor FIM Effectiveness of 21.1±21.9 (−5-57). In contrast, among the 48 patients without a history of heart disease (48/57 patients), the Motor FIM score at admission was 37.3±17.0 (13-71) and the Motor FIM score at discharge was 69.4 ±24.2 (14-91), with a Motor FIM Effectiveness of 32.2±20.2 (0-77). There was a tendency for the Motor FIM Effectiveness and Motor FIM scores to be lower in the group with a history of heart disease, only the Motor FIM score at discharge exhibited statistical significance. This is attributed to the psychological bias of the therapist regarding the patient's history of heart disease before admission and throughout their hospitalization at TGRH. As a result, the exercise load was insufficient compared to other patients, resulting in poor recovery of activity and the living environment.

This study has several limitations. The first limitation of this study is the insufficient number of cases. Because of the small number of cases, factor analysis could not be performed and inhibitory factors could not be identified. As this study investigated cases within the convalescence ward of a single facility, it cannot be concluded that the sample size was adequate to definitively demonstrate the effectiveness of rehabilitation in the post-acute phase. However, the convalescence ward is an integral part of the medical system in Japan, with numerous convalescence wards across the country admitting patients with post-acute phase COVID-19 pneumonia, similar to this study. Integrating data from these convalescence wards could potentially address the issue of insufficient case numbers and enable valid factor analysis. Second, there is a potential bias in the cases. Specifically, the participants of this study were limited to individuals with COVID-19 pneumonia who required admission to acute hospitals, treatment was administered under confinement., had FIM scores of 115 or below, and for whom returning home was deemed difficult. Individuals with post-acute phase COVID-19 pneumonia who did not require hospitalization were excluded, introducing a bias when

evaluating the effectiveness of rehabilitation for these cases. Third, the study did not investigate symptoms that persist over an extended period, also known as long COVID. A systematic review by Nasserie et al of 45 studies, encompassing 9751 cases, indicated that the median prevalence of individuals experiencing at least one persistent symptom (such as dyspnea, fatigue, insomnia, anosmia, and dysgeusia) lasting ≧60 days from diagnosis/onset/hospitalization or ≧30 days from discharge/recovery was 72.5%[16]. Although the hospitalization period for the participants in this study included the duration of these persistent symptoms, no systematic investigation was conducted, and dysgeusia was confirmed in only one case. Therefore, future studies should explore these persistent symptoms further to gain a deeper understanding.

This study investigated the effectiveness of rehabilitation for COVID-19 Pneumonia patients in a convalescence ward. Rehabilitation was found to be effective, enhancing activity levels and potentially maintaining or improving the living environment after discharge. A factor inhibiting this was identified as low activity during admission to the convalescence ward, suggesting the usefulness of rehabilitation during the acute phase. In addition, this study suggests that exercise load may be insufficient in patients with a history of heart disease, resulting in poor recovery of activity and living environment.

One of the limitations of this study is the small sample size, which precluded factor analysis. Furthermore, the investigation did not encompass Long COVID. To address these limitations, we intend to promote multi-center research and re-evaluate the survey items.

Acknowledgements

All authors have no COI to declare regarding this study.

References

1. Curci C, Pisano F, Bonacci E, et al. Early rehabilitation in post-acute COVID-19 patients: data from an Italian COVID-19 Rehabilitation Unit and proposal of a treatment protocol. Eur J Phys Rehabil Med 2020;56:633-641.
2. Curci C, Negrini F, Ferrillo M, et al. Functional outcome after inpatient rehabilitation in postintensive care unit COVID-19 patients: findings and clinical implications from a real-practice retrospective study. Eur J Phys Rehabil Med 2021;57:443-450.
3. Zampogna E, Paneroni M, Belli S, et al. Pulmonary rehabilitation in patients recovering from COVID-19. Respiration 2021;100:416-422.
4. Al Chikhanie Y, Veale D, Schoeffler M, et al. Effectiveness of pulmonary rehabilitation in COVID-19 respiratory failure patients post-ICU. Respir Physiol Neurobiol 2021;287:103639.
5. Spielmanns M, Pekacka-Egli AM, Schoendorf S, et al. Effects of a comprehensive pulmonary rehabilitation in severe post-COVID-19 patients. Int J Environ Res Public Health 2021;18:2695.
6. R Core Team (2020). R: A language and environment for statistical computing. R Foundation for statistical computing, Vienna, Austria, https://www.R-project.org/
7. Matsunaga N, Hayakawa K, Terada M, et al. Clinical epidemiology of hospitalized patients with coronavirus disease 2019 (COVID-19) in Japan: report of the COVID-19 Registry Japan. Clin Infect Dis 2021;73:e3677-e3689.
8. Tanaka C, Tagami T, Nakayama F, et al. Association between mortality and age among mechanically ventilated COVID-19 patients: a Japanese nationwide COVID-19 database study. Ann Intensive Care 2021;11:171.
9. Asai Y, Nomoto H, Hayakawa K, et al. Comorbidities as risk factors for severe disease in hospitalized elderly COVID-19 patients by different age-groups in Japan. Gerontology 2022;68:1027-1037.
10. Patelli G, Paganoni S, Besana F, et al. Preliminary detection of lung hypoperfusion in discharged COVID-19 patients during recovery. Eur J Radiol 2020;129:109121.
11. Mo X, Jian W, Su Z, et al. Abnormal pulmonary function in COVID-19 patients at time of hospital discharge. Eur Respir J 2020;55:2001217.
12. You J, Zhang L, Ni-Jia-Ti MY, et al. Anormal pulmonary function and residual CT abnormalities in rehabilitating COVID-19 patients after discharge. J Infect 2020;81:e150-e152.

13. Barker-Davies RM, O'Sullivan O, Senaratne KPP, et al. The Stanford Hall consensus statement for post-COVID-19 rehabilitation. Br J Sports Med 2020;54:949-959.
14. Ceravolo MG, de Sire A, Andrenelli E, et al. Systematic rapid "living" review on rehabilitation needs due to COVID-19: update to March 31st, 2020. Eur J Phys Rehabil Med 2020;56:347-353.
15. Ikebuchi M, Ohta Y, Minoda Y, et al. Efficacy of early rehabilitation for severe coronavirus disease 2019 pneumonia: factor analysis using machine learning. Prog Rehabil Med 2023;8:20230027.
16. Nasserie T, Hittle M, Goodman SN, Assessment of the frequency and variety of persistent symptoms among patients with COVID-19: a systematic review. JAMA Netw Open 2021;4:e2111417.

Osaka City Med. J. Vol. 72, 11-16, 2026

Strategy for Treatment of Patients with Severe COVID-19 Pneumonia at Osaka Metropolitan University Hospital: Findings from Treatment Experience

Hiromichi Fujii[1], Shoichi Ehara[1], Hiroshi Kakeya[2],
Yasumitsu Mizobata[3], and Toshihiko Shibata[4]

Departments of Intensive Care Medicine[1], Infection Control Science[2], Traumatology and Critical Care Medicine[3], and Cardiovascular Surgery[4], Graduate School of Medicine, Osaka Metropolitan University

Abstract

Background

During the COVID-19 pandemic, Osaka Metropolitan University Hospital treated patients with severe COVID-19 pneumonia. While the prone position is known to improve oxygenation in patients with acute respiratory distress syndrome, its implementation requires many medical staff members. Due to the increasing number of COVID-19 cases among healthcare staff, maintaining patients in the prone position became difficult. To address this issue, the semi-prone (Sims) position was introduced as an alternative.

Methods

This study compared two patient groups: Group A, comprising 56 patients treated in July to November 2021; and Group B, comprising 31 patients treated in January to April 2022. The study further compared 29 patients in Group A who received prone position treatment (Group A-p) and 16 patients in Group B who were eligible for prone position treatment but received Sims position treatment (Group B-s). Key outcomes, including extubation rates, patient transfers, and mortality, were analyzed.

Results

No significant differences were observed in the extubation and transfer rates between Group A and Group B. The subgroup analysis that compared patients in Group A-p and patients in Group B-s found no significant differences in the outcomes, despite worse respiratory conditions in Group B-s.

Conclusions

The Sims position could potentially serve as an alternative to the prone position in managing patients with severe COVID-19 pneumonia, especially when medical resources are limited. Further

Received April 10, 2025; accepted June 10, 2025.
Correspondence to: Hiromichi Fujii, MD, PhD.
Department of Intensive Care Medicine, Graduate School of Medicine, Osaka Metropolitan University, 1-4-3 Asahimachi, Abeno-ku, Osaka 545-8585, Japan
Tel: +81-6-6645-3993; Fax: +81-6-6645-3071
E-mail: fujiihiro@omu.ac.jp

research is needed to validate its efficacy in broader intensive care settings. These findings provide valuable insights for optimizing respiratory management strategies during future pandemics.

Key Words: COVID-19; Severe pneumonia; Prone position; Sims position

Introduction

In Japan, the number of coronavirus disease 2019 (COVID-19) cases increased following the discovery of COVID-19 on a luxury cruise ship in 2020[1,2]. In Osaka Metropolitan University Hospital, we treated patients with severe COVID-19 pneumonia. The doctors in the Trauma and Critical Care Center at our hospital treated patients with severe COVID-19 pneumonia during the first year of the pandemic. However, the management of patients with marked hypoxia requires many medical staff members. Therefore, from April 2021, a dedicated treatment team for COVID-19 patients was formed from almost all departments in the hospital.

The effectiveness of early neuromuscular blocker administration and the prone position in patients with severe acute respiratory distress syndrome (ARDS) has been reported[3,4], and thus we administered muscle relaxants and prone position treatment for patients with severe COVID-19 pneumonia as soon as possible. However, managing patients in the prone position requires many staff members and high expertise[5]. At the same time as COVID-19 cases outside the hospital were markedly increasing, the number of infected staff members in the hospital was also markedly increasing. Consequently, it became difficult to secure sufficient staff to safely manage the prone position for COVID-19 patients. Semi-prone position (Sims) position is a side-lying posture that approximates the prone position, with the patient lying on the left side and the right leg flexed, which can be managed by a small number of nursing staff. We considered that the Sims position, a posture resembling the prone position, may offer comparable effectiveness. Therefore, instead of the prone position, we decided to actively use the semi-prone (Sims) position.

In this article, we describe our experience with the Sims position at Osaka Metropolitan University Hospital for the treatment of COVID-19 patients and compare the prone position with the Sims position.

Methods

Among the patients treated by the COVID-19 treatment team at Osaka Metropolitan University Hospital, we investigated the prognosis of 56 patients in Group A treated between July and November 2021 (so-called fifth wave in Japan) and 31 patients in Group B treated between January and April 2022 (so-called sixth wave)[6]. During the Group A period, the medical staff was less prevalently affected by COVID-19 and the prone position could be actively maintained. During the Group B period, COVID-19 was prevalent among the medical staff, and many staff were unable to come to work. Therefore, the Sims position was used instead of the prone position. Both groups of patients were intubated and managed with continuous administration of muscle relaxants for at least 2 days to suppress spontaneous breathing and to care for lung protective ventilation. Since our hospital was a treatment hospital for patients with severe COVID-19 pneumonia, all patients who could be extubated were transferred to other hospitals. Stable patients with tracheotomy were also transferred. Hence, each patient's prognosis was determined by whether they could be transferred or died in the hospital. We investigated the prognosis and the number of extubation cases between the two groups.

This study was approved by the institutional ethics committee at Osaka Metropolitan University Hospital (approval no. 2022-076).

Prone position and Sims position

For the prone position, the patient was placed in that position for at least 16 hours from approximately 6 p.m. to 10 a.m. the next day, with 5-6 staff members carefully floating the body to change the face orientation every 4 hours and prevent the intubation tube from falling out. During the day, position changes were performed in the Sims, supine, and lateral positions. For the Sims position, the patient was placed in that position with either the left or right side of the body facing down, and the arm that would be under the body was placed in a semi-prone position, rather than being taken to the dorsal side.

Indications for the prone position

The indications for the prone position were obesity (body mass index [BMI] >25 kg/m^2), PaO2/FiO2 (P/F) ratio after intubation <150, or extensive inflammation mainly on the dorsal side, such as type H described by Gattinoni et al[7], on chest CT. In Group B, some patients were actively exchanged for the left and right positions in the Sims position even if they matched the criteria for the prone position. The 29 patients who received prone position treatment in Group A were grouped as Group A-p, and the 16 patients who were indicated for prone position treatment but received Sims position treatment in Group B were grouped as Group B-s. We also compared the results between these two groups.

Statistical analysis

Categorical variables are presented as counts, and continuous variables are presented as medians with interquartile ranges. The chi-square test was used to compare categorical variables, and the Mann-Whitney U test was applied to continuous variables to evaluate differences between Group A and Group B, as well as between Group A-p and Group B-s.

Differences were considered significant at $p<0.05$. All statistical analyses were performed using SPSS version 29 (IBM Corp., Armonk, NY, USA).

Results

During the study period, antiviral drugs, corticosteroids, immunomodulators, and anticoagulant therapy were routinely administered to patients with severe respiratory failure due to COVID-19, including those in groups A and B of this study. No adverse events related to ventilation in the prone or Sims position was observed in this study.

The factors compared between Group A and Group B were sex, age, weight, BMI, and P/F ratio after intubation, Sequential Organ Failure Assessment (SOFA) score at admission, Acute Physiology And Chronic Health Evaluation Version Ⅱ (APACHE Ⅱ) score at admission, presence of extubation, and prognosis.

As shown in Table 1, 29 of the 56 patients in Group A were treated in the prone position, while no patients in Group B were treated in the prone position. Significant differences between Group A and Group B were noted for age, weight, BMI, number of patients with BMI >25 kg/m^2, and APACHE Ⅱ score at admission. The patients in Group A were younger and more obese than those in Group B. There was no difference in the SOFA scores between the two groups, but the APACHE Ⅱ score was lower in Group A than in Group B. The P/F ratios did not differ significantly between the two groups, indicating that there was no difference in the respiratory status between the two groups.

Table 1. Patient characteristics

	Group A	Gorup B	p-value
male/female	48/8	25/6	0.537
age	53 (47.5-60.5)	74 (61.5-78)	<0.001
weight (kg)	71 (59.9-88.4)	64 (53.5-69.0)	0.005
BMI (kg/m^2)	24.9 (21.7-29.2)	23.1 (20.2-24.9)	0.046
BMI >25 (case)	27	8	0.041
P/F ratio	202 (150-282)	172 (118-254)	0.298
SOFA score	3 (2-5)	4 (3-5.5)	0.101
APACHE Ⅱ score	10 (7-13)	14 (10-17)	0.003
prone position	29	0	

	Group A-p	Gorup B-s	p-value
male/female	26/3	12/4	0.194
age	52 (45-56)	74 (66.5-76)	<0.001
weight (kg)	76.4 (67.3-93.9)	65.6 (54.8-69.3)	0.002
BMI	28.0 (23.8-30.9)	21.1 (22.4-27.9)	0.079
BMI >25	18/11	7/9	0.237
P/F tatio	190 (139-273)	127 (96.5-165)	0.007
SOFA score	3 (2-5)	4 (3-6)	0.084
APACHE Ⅱ score	10 (7-13)	14 (11.8-20)	0.002

BMI, body mass index; P/F, PaO2/FiO2; SOFA, Sequential Organ Failure Assessment; and APACHE Ⅱ, Acute Physiology And Chronic Health Evaluation Version Ⅱ.

Table 2. Patient outcomes by groups

	Group A	Gorup B	p-value
extubation/no exatubation	44/12	23/8	0.642
hospital transfer/dead	51/5	25/6	0.161

	Group A-p	Gorup B-s	p-value
extubation/no exatubation	23/6	10/6	0.222
hospital transfer/dead	25/3	12/4	0.347

We also compared the results between Group A-p (29 patients) who received prone position treatment and Group B-s (16 patients) who were indicated for prone position treatment but received Sims position treatment. Significant differences between Group A-p and Group B-s were noted for age, weight, P/F ratio, and APACHE Ⅱ score. The patients in Group A-p were younger and heavier than those in Group B-s, but there was no difference in BMI. The F/P ratio was higher in Group A-p than in Group B-s, and the patients in Group B-s had worse respiratory conditions.

Table 2 shows the results for the prognosis of the patients based on the presence of extubation and the numbers of transfers or deaths. No significant differences were found in the numbers of hospital transfers or deaths and the presence of extubation between Group A and Group B. There were also no significant differences between Group A-p and Group B-s.

Discussion

Our hospital is a university hospital that was assigned to treat patients with severe COVID-19 pneumonia. Initially, COVID-19 patients were treated in the Trauma and Critical Care Center at the hospital. However, as the number of COVID-19 patients increased, there was a limit to how many patients could be treated by one department. Therefore, it was decided that almost all departments at the hospital would cooperate to form a COVID-19 treatment team to deal with these patients.

At first, the internal medicine department was providing assistance to another hospital in Osaka City, and thus the team was formed by the surgical department with cardiovascular surgeons as the main members. The first COVID-19 team consisted of all cardiovascular surgeons and one each from respiratory surgery and anesthesiology. A ward was set up for COVID-19 patients, and treatment was started from the so-called third wave in Japan. Finally, doctors from the internal medicine department also joined the team to provide treatment. It was very difficult to obtain doctors for the COVID-19 team without stopping the University Hospital service. However, during the first 6 weeks, all of the cardiovascular surgeons treated COVID-19 patients without performing surgery.

The PROSEVA study found that prone position treatment led to a better prognosis for ARDS patients when performed for ≧16 hours in patients with P/F ratio ＜150[4]. It was also reported that oxygenation was enhanced in the prone position for COVID-19 patients, and that oxygenation became increasingly better as the placing of the patient in the prone position became earlier[8]. Meanwhile, early administration of neuromuscular blockers to control spontaneous breathing was reported to improve the prognosis of ARDS patients[3]. Therefore, during the Group A period in our hospital, we actively used the prone position with early administration of neuromuscular blockers for treatment of COVID-19 patients with the appropriate indications.

However, careful management of patients under deep sedation in the prone position is necessary due to the risks of airway tube obstruction, pressure ulcers on the face and chest, nerve damage due to limb compression, and hemodynamic instability. Therefore, prone position treatment requires the ability to reorient the face every 4 hours and cope with hemodynamic instability. This means that both doctors and nurses need to be competent and proficient, and a small number of medical staff is insufficient. This does not mean that it is difficult to change the supine position to the prone position, rather that it is difficult to manage a patient in the prone position. While it has not proven difficult to manage one ARDS patient in the prone position in the intensive care unit under normal circumstances, it was difficult to manage several COVID-19 patients in the prone position every day during the COVID-19 pandemic.

The Sims position, also known as the gynecological position[9], is closer to the prone position than the lateral position. An advantage of the Sims position is that it is easy to change the body position, even at night, because the position changes can be performed by only a few nurses. Furthermore, the patient can easily be placed in the supine position, so that the position can be returned as necessary during the day when there are many examinations.

During the Group A period (so-called fifth wave), there were not many infected staff members in the hospital, and thus patients in the prone position could be actively managed. However, during the Group B period (so-called sixth wave), the number of infected patients nationwide rose sharply (https://www.mhlw.go.jp/content/10900000/001010896.pdf), and the number of infected hospital staff members also increased markedly, making it difficult to secure sufficient staff numbers. Consequently, the prone position, which requires many staff, could no longer be actively managed.

Therefore, during the Group B period, patients were actively placed in the Sims position, which can be managed by only two or three nurses, rather than in the prone position.

In this study, the prognosis of the Group A-p patients who were actively managed in the prone position was compared with that of the Group B-s patients who were managed in the Sims position. In particular, although patients in the B-s group had poorer respiratory status and higher APACHE Ⅱ score than those in the A-p group, there was no significant difference in the numbers of death or patients who could be extubated in Group B-s compared with Group A-p. Given the minimal human resources required for the Sims position, it may represent a practical non-invasive ventilation strategy for patients with severe respiratory failure in ICUs with limited staffing. However, the present study has some limitations that require consideration. Briefly, the study had a small number of cases, given that it only investigated patients with severe COVID-19 pneumonia, and compared two groups at different epidemic periods containing 56 and 31 patients. Future studies are warranted to investigate whether the present findings will hold true for ARDS patients in intensive care units.

During the COVID-19 pandemic, we treated patients with severe COVID-19 pneumonia at our hospital. The treatment of these patients by a team of doctors selected from almost all departments was a unique feature of our hospital. The findings indicate a potential role for the Sims position as an alternative to the prone position in the management of patients with severe COVID-19 pneumonia. These findings may be useful in the response to future infectious disease pandemics.

Acknowledgments

All authors have no COI to declare regarding the present study.

The authors thank Alison Sherwin, PhD, from Edanz (https://jp.edanz.com/ac) for editing a draft of this manuscript.

Reference

1. Tsuboi M, Hachiya M, Noda S, et al. Epidemiology and quarantine measures during COVID-19 outbreak on the cruise ship Diamond Princess docked at Yokohama, Japan in 2020: a descriptive analysis. Glob Health Med 2020;2:102-106.
2. Hayakawa K, Asai Y, Matsunaga N, et al. Evaluation of the representativeness of data in the COVID-19 Registry Japan during the first six waves of the epidemic. Glob Health Med 2022;4:204-209.
3. Papazian L, Forel JM, Gacouin A, et al. Neuromuscular blockers in early acute respiratory distress syndrome. N Engl J Med 2010;363:1107-1116.
4. Guérin C, Reignier J, Richard JC, et al. Prone position in severe acute respiratory distress syndrome. N Engl J Med 2013;368:2159-2168.
5. Lucchini A, Bambi S, Mattiussi E, et al. Prone position in acute respiratory distress syndrome patients: a retrospective analysis of complications. Dimens Crit Care Nurs 2020;39:39-46.
6. Kobayashi M, Miyamoto A, Watanabe T, et al. COVID-19 vaccination benefits in preventing severe disease in mild-to-moderate cases: an analysis in the first specialized hospital for COVID-19 in Japan. Respir Investig 2023;61:230-239.
7. Gattinoni L, Chiumello D, Caironi P, et al. COVID-19 pneumonia: different respiratoy treatments for different phenotypes? Intennsive Care Med 2020;46:1099-1102.
8. Coppo A, Bellani G, Winterton D, et al. Feasibility and physiological effects of prone positioning in non-intubated patients with acute respiratory failure due to COVID-19 (PRON-COVID): a prospective cohort study. Lancet Respir Med 2020;8:765-774.
9. Wall LL. The Sims position and the Sims vaginal speculum, re-examined. Int Urogynecol J 2021;32:2595-2601.

Osaka City Med. J. Vol. 72, 17-27, 2026

Effects of a Pulsatile Flow Generator Using a Solenoid Valve on Rabbit Myocardial Perfusion

Yukihiro Nishimoto[1)], Shuji Inamori[1, 2)], Yasunori Yamasaki[2)],
Toshihiko Shibata[1)], and Yosuke Takahashi[1)]

Department of Cardiovascular Surgery[1)],
Graduate School of Medicine, Osaka Metropolitan University; and
Department of Medical Engineering[2)], Faculty of Health Science, Aino University

Abstract

Background

Venoarterial extracorporeal membrane oxygenation (VA-ECMO) is essential in cardiac surgery and cardiogenic shock management. ECMO generally uses centrifugal pumps; of which blood flow is nonpulsatile, and organ perfusion is nonphysiological. The methods for generating pulsatile flow include changing the rotation rate of the roller pump or using intra-aortic balloon pumping (IABP). We developed a pulsatile flow generator with a solenoid valve (K-Beat) that can be incorporated into VA-ECMO using an existing centrifugal pump. In this study, we observed the effects of pulsatile flow on myocardial perfusion in medium-sized rabbits.

Methods

First, as a preliminary experiment, the IABP and K-Beat were installed in a simulated circuit, and the characteristics of the pulsatile pressure generated by these devices were measured. Next, six rabbits were subjected to extracorporeal circulation using VA-ECMO with K-Beat insertion. Myocardial perfusion in the inferior wall of the left ventricle, lateral wall of the left ventricle, and anterior wall of the right ventricle was measured immediately after ECMO initiation, 30 min later, and 60 min later.

Results

In a simulated circuit experiment, the K-Beat generated a pulsatile pressure equivalent to or greater than that of the IABP. In experiments with rabbits, myocardial perfusion increased significantly more when the K-Beat was turned on than when it was turned off at all time phases and regions. This effect was more pronounced when autocardiac output was weakened.

Conclusions

A pulsatile flow generator with a solenoid valve could easily be installed in an existing VA-ECMO system using a centrifugal pump to increase myocardial perfusion. Experiments using larger animals

Received May 28, 2025; accepted November 25, 2025.
Correspondence to: Yukihiro Nishimoto, MD.
Department of Cardiovascular Surgery, Graduate School of Medicine, Osaka Metropolitan University,
1-4-3 Asahimachi, Abeno-ku, Osaka 545-8585, Japan
Tel: +81-6-6645-3980; Fax: +81-6-6646-3071
E-mail: nishimoto_yukihuro@yahoo.co.jp

to generate pulsatile flow for longer periods should be conducted to verify the effects on other organs.

Key Words: Extracorporeal circulation; Pulsatile perfusion; Rabbit

Introduction

Venoarterial extracorporeal membrane oxygenation (VA-ECMO) is essential for cardiac surgery and cardiogenic shock care in cardiovascular surgery, cardiology, and intensive care medicine. VA-ECMO generally requires relatively little hemolysis, even when driven at high flow rates for long periods, and centrifugal pumps are widely used as the driving devices. However, centrifugal pumps produce only nonpulsatile flows. Loss of pulsatile pressure causes vascular endothelial damage and decreases nitric oxide production, which may lead to the deterioration of organ perfusion[1-4]. Therefore, the 2019 European Association for Cardio-Thoracic Surgery/European Association of Cardio-Thoracic Anesthesiology)/European Board of Cardiovascular Perfusion guidelines for artificial hearts and lungs in adult cardiac surgery[5] state that pulsatile flow may reduce postoperative pulmonary and renal complications and should be considered for patients at a high risk of poor pulmonary and renal outcomes (recommendation level: class Ⅱa). The methods for generating pulsatile flow include periodically varying the rotation speed of the roller pump and intra-aortic balloon pumping (IABP)[6]. However, methods that use a roller pump are difficult to synchronize with a patient's electrocardiogram (ECG), and high rotation and prolonged use can cause hemolysis. In addition, the IABP method involves invasive balloon insertion, access route problems, and risk of lower extremity ischemia[7]. To solve these problems, Inamori et al developed a completely new pulsatile flow generator that uses a solenoid valve to compress and release the pillow in synchronization with the ECG and named it K-Beat (patent no. 5557175) (Fig. 1). Furthermore, this device can be installed in VA-ECMO using an ordinary centrifugal pump. Inamori et al[8] used the K-Beat during selective cerebral perfusion in rats and demonstrated that pulsatile flow is superior to nonpulsatile flow in cerebral microvascular perfusion. Fujii et al[9] have demonstrated that the K-Beat can be used with VA-ECMO to produce effective pulsatile flow in pigs. However, the effect of pulsatile flow on organ–tissue perfusion remains unclear. Thus, this study aimed to investigate the effects of pulsatile flow on myocardial perfusion in medium-sized rabbits.

Structure of pulsatile flow generator

The pulsatile flow generator (K-Beat) installs a pillow into the arterial route of the VA-ECMO and consists of a solenoid valve that compresses and releases it, a pillow fixator, and a control unit (Fig. 1). The pillow fixator has a screw to adjust the depth to which the pillow is compressed. Although hemolysis unlikely occurs when positive pressure is applied, it can occur easily when negative pressure is applied[10]. Because only pressure is applied by the solenoid valve and the pillow is opened only by the elasticity of the pillow, excessive negative pressure is absent, and hemolysis can be minimized. It can also be easily integrated into existing VA-ECMO devices.

The timing of ECG synchronization is sent to the delay circuit when the controller detects the R wave (systole) on the ECG, and the solenoid valve is turned on at the time of the T wave to compress the pillow and generate pulse pressure, which is then released during systole (Fig. 2). This reduces the afterload during autocardiac systole and increases the coronary blood flow during diastole, as in IABP. The timing and duration of the compression can be fine-tuned, and by using a solenoid valve with a low time loss, following the heart rate up to approximately 200 bpm is possible. Furthermore, this device can be operated at a set number of times; therefore, it can be used as a pulsatile flow

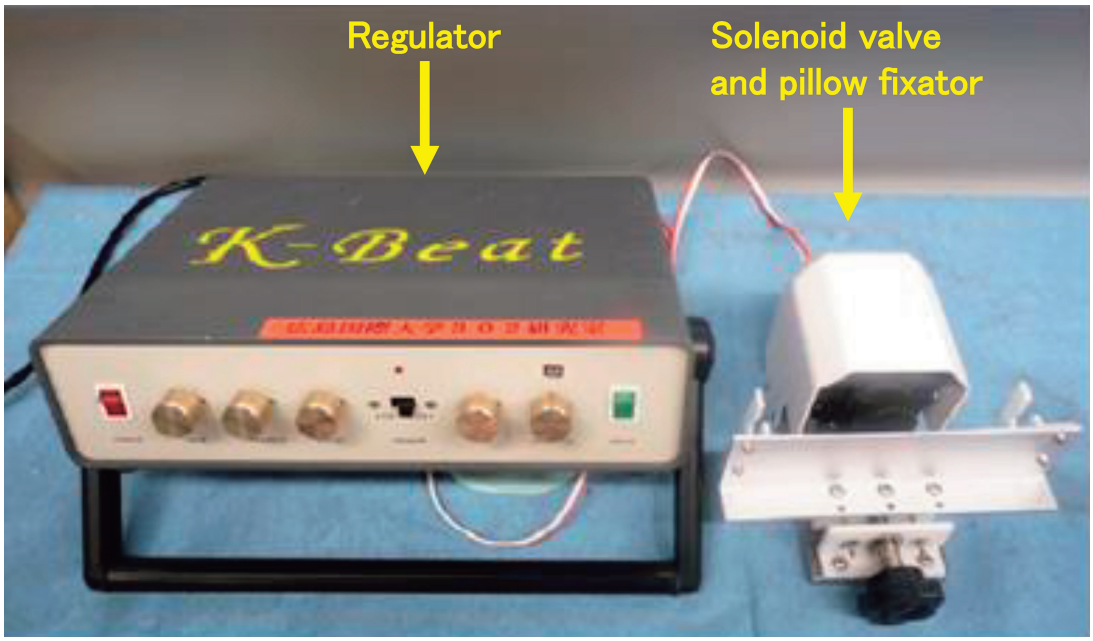

Figure 1. Pulsatile flow generator "K-Beat".
This device consists of a solenoid valve with a control device that controls the timing and duration of compression in synchronization with the electrocardiogram, and a pillow with a fixed device that can adjust the depth of compression.

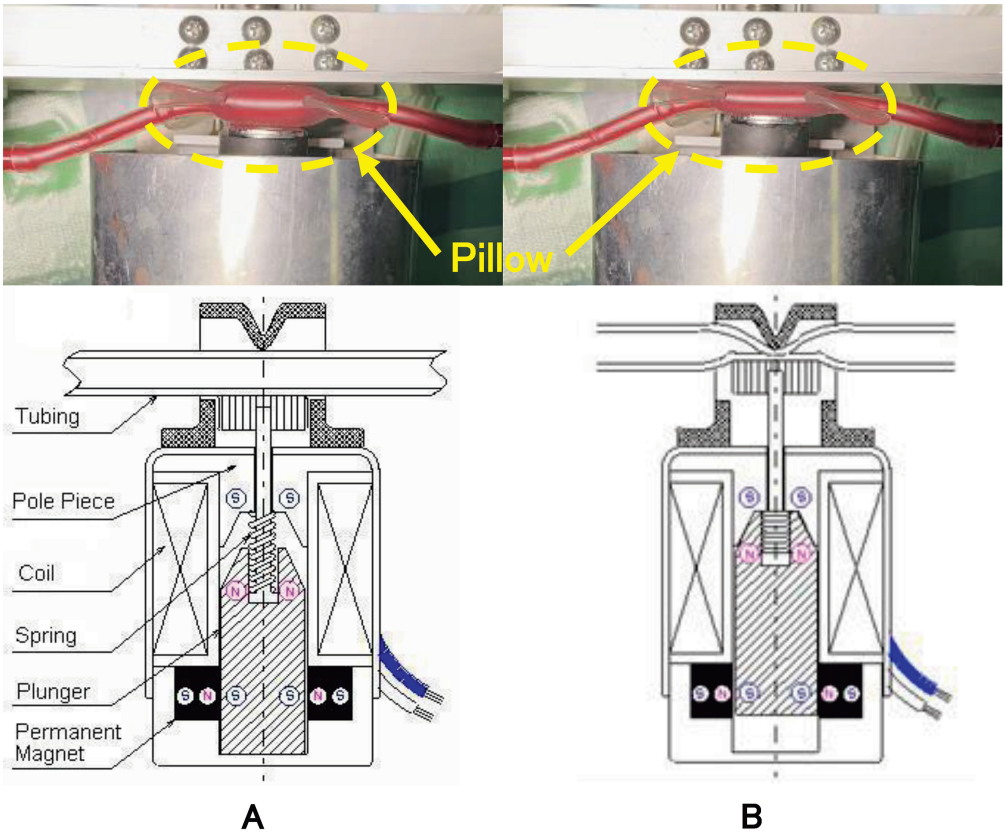

Figures 2. Close view of the pillow and mechanism of the solenoid valve.
A. When the solenoid valve is turned on, the electromagnetic force is generated to push the pole piece, and the pillow is compressed.
B. When the solenoid valve is turned off, the solenoid valve returns automatically owing to the permanent magnet, and the pillow is released.

generator even during cardiac arrest, when ECG synchronization is impossible.

A normal solenoid valve requires electric power to maintain the open state. The device uses a latching mechanism with a permanent magnet to keep the valve open (Fig. 2). The use of a permanent magnet eliminates the need for electric power to keep the valve open, thereby reducing associated heat generation. The temperature of devices used in the medical field is limited to a maximum of 42℃ to prevent hemolysis.

Methods

Simulation circuit

The IABP or K-Beat was attached to the arterial route of the VA-ECMO, and the pulsatile pressure was measured under constant flow (2.0 L/min) at 60 bpm (n=5 for each). Pulsatile pressure was defined as the difference between the highest and lowest pressures. The console was a STOCKERT SCPC® (Livanova, Milan, Italy), the circuit was HPO-06H-C® (Senko Medical Instrument, Tokyo, Japan, 450 mL filling volume), and the centrifugal pump was a MIX flow 3® (JMS, Hiroshima Japan). To ensure biological conditions, a saline solution with glycerol was used as the filling solution to achieve a viscosity of 4.3 cp. The mean arterial pressure during the VA-ECMO operation was approximately 40 mm Hg, a column of mercury was converted to a column of water, and the blood supply connection of the simulated reservoir was placed 54 cm below the liquid level.

1. Simulated circuit with IABP

A bifurcated connector with a diameter of 10-10-10 mm was attached to the middle of the VA-ECMO arterial route. A 25-cm balloon of IABP (corart BP1-V AISIN®, Senko Medical Instrument) was inserted through one end of the connector, and the insertion point was sealed with a rubber

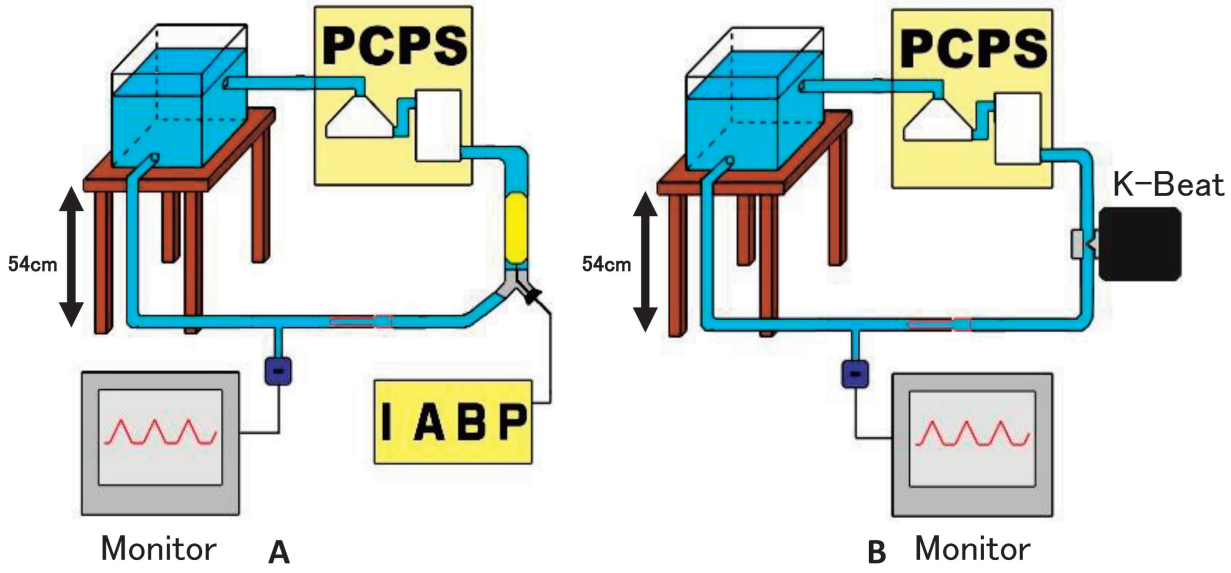

Figures 3. Simulation circui.

A. A bifurcated connector was attached to the middle of the VA-ECMO blood supply route, and an IABP balloon was inserted at one end.

B. A K-Beat solenoid valve and a 35-mL pillow were incorporated in the middle of the blood delivery route of the VA-ECMO.

VA-ECMO, venoarterial extracorporeal membrane oxygenation; and IABP, intra-aortic balloon pumping.

stopper. The tube diameter was 0.5 inch (approximately 10 mm), so the effective volume of the beating balloon volume was 19.6 mL (Fig. 3A).

2. Simulated circuit with the K-Beat

A K-Beat solenoid valve was installed in the middle of the VA-ECMO arterial route and was set to operate at 60 bpm. The VA-ECMO blood delivery flow rate was set to 2.0 L/min. A 35-mL pillow was installed in the arterial route, and the experiment was performed (Fig. 3B).

Animal experiment

1. Animals

Six male New Zealand White rabbits weighing 3.0-3.5 kg each were used. Animal experiments were approved by the Animal Experiment Committee of Osaka Metropolitan University (23075).

2. Surgical procedure

Each rabbit was placed in a box filled with 5 L/min of O_2 and 5% isoflurane, and anesthesia was induced. Once the rabbit fell asleep, it was placed in the supine position, the gas circuit was switched from the box to the mask, and anesthesia was maintained with isoflurane. The neck, abdomen, and groin were shaved, and the counter electrode of an electric scalpel was applied. Tracheostomy was performed, and an 8 Fr tracheal tube was inserted and connected to a ventilator (SN-480-7, Shinano Seisakusho, Tokyo, Japan). After connecting to the ventilator, O_2 was reduced to 1 L/min, and isoflurane was reduced to 3%. The ventilator settings were set to a tidal volume of 10 mL/kg and respiratory rate of 30 breaths/min. End-tidal pressure was measured and maintained below 10 cmH_2O.

An incision was made in the right groin, and a 22 G catheter was inserted into the common femoral vein for venous access. A laparotomy was performed, and a 22 G catheter was inserted into the abdominal aorta via the right common iliac artery, followed by invasive blood pressure measurement. A median sternotomy was performed, and the bifurcation of the brachiocephalic artery (BCA), left common carotid artery (LCCA), and left subclavian artery (LSCA) was exposed. The distal sides of the LCCA and LSCA were ligated, and the bifurcation was cut to allow the insertion of a 14 G catheter into the BCA, which was used as the arterial cannula. The pericardium was incised, and a 12 Fr malleable single-stage DLP vein cannula (Medtronic, Dublin, Ireland) was inserted into the right atrial appendage to establish extracorporeal circulation (Fig. 4). The VA-ECMO console, circuit, and centrifugal pump were identical to those used for the simulated circuit.

The K-Beat was applied at three time points (immediately after the initiation of extracorporeal circulation, 30 min later, and 60 min later), and changes in myocardial perfusion (mL/min/100g) in the inferior wall of the left ventricle (IWLV), lateral wall of the left ventricle (LWLV), and anterior wall of the right ventricle (AWRV) were measured using a laser tissue blood flow meter (ALF 21®, Admedec, Tokyo, Japan). After the experiment, the VA-ECMO was turned off, and the rabbits were euthanized.

Statistical analysis

The results of the simulated circuit did not follow a normal distribution. A *t*-test was used to compare two unrelated groups. The results of the animal experiments also did not follow a normal distribution. The Wilcoxon signed-rank test was used to compare two related groups using the same individuals. The EZR version 4.3.1 was used for all statistical analyses.

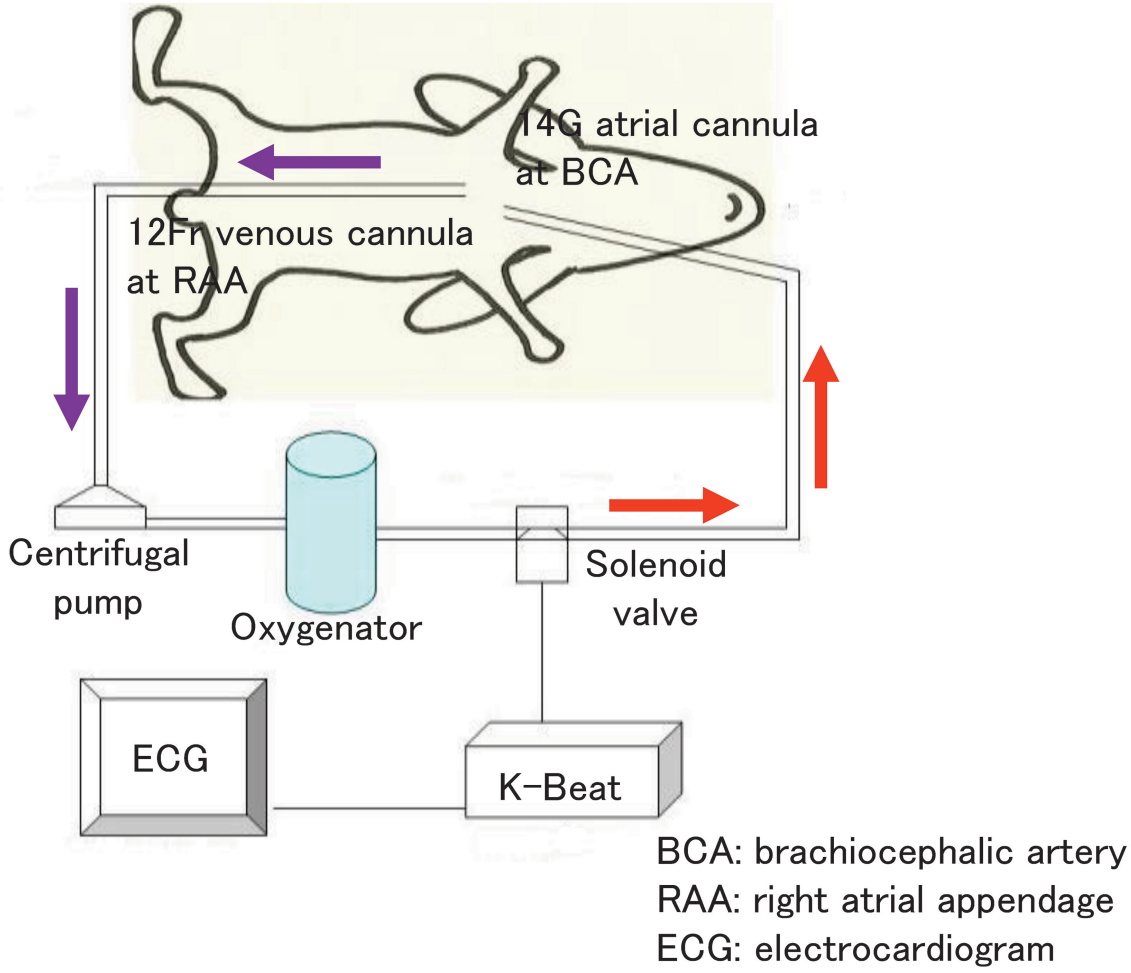

Figure 4. Schema of cardiopulmonary bypass applied on a rabbit.
New Zealand White male rabbits weighing 3.0-3.5 kg were used. A 14 G arterial cannula was inserted into the BCA, and a 12 Fr venous cannula was inserted into the right atrial appendage. A solenoid valve and pillow were installed in the middle of the arterial route. The solenoid valve was regulated by the K-Beat synchronized with the ECG. BCA, brachiocephalic arter; and ECG, electrocardiogram.

Results

Simulated circuit

In the experiments using a simulated circuit installing IABP or K-Beat, the pulsatile pressure (mm Hg) generated using an arterial cannula of 16 Fr, 18 Fr, and 20 Fr was [IABP 34-36 (mean 31.7, interquartile range [IQR] 5.75) vs K-Beat 38-40 (mean 34.8, IQR 6.75), p=0.000122]; [IABP 37-39 (mean 34.8, IQR 6.75) vs K-Beat 36-39 (mean 34.3, IQR 6.75), p=0.373000]; and [IABP 34-37 (mean 33.0, IQR 5.75) vs K-Beat 40-43 (mean 37.8, IQR 7.25), p=0.000042], respectively (Fig. 5).

Animal experiment

1. Pulsatile flow generation

The K-Beat synchronized with the ECG, even at a heart rate of 160 bpm. Diastolic blood pressure (diastolic augmentation) increased, whereas systolic blood pressure (systolic unloading) decreased (Figs. 6A and 6B).

2. Myocardial perfusion

At 0 min, the myocardial perfusion (mL/min/100g) for the IWLV, LWLV, and AWRV was [K-Beat

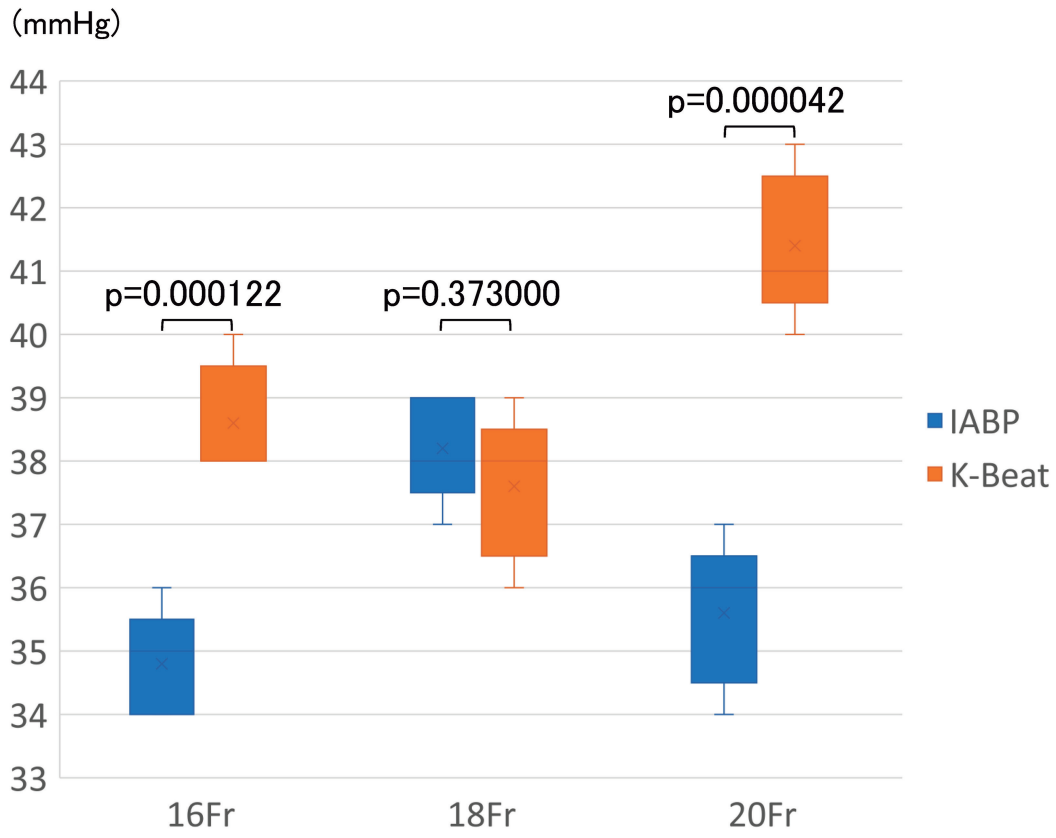

Figure 5. Pulsatile pressure generated by IABP vs K-Beat in the simulation circuit.

The pulsatile pressure was [34-36 (mean 31.7, IQR 5.75) vs 38-40 (mean 34.8, IQR 6.75), p=0.000122; [37-39 (mean 34.8, IQR 6.75) vs 36-39 (mean 34.3, IQR 6.75), p=0.373000]; and [34-37 (mean 33.0, IQR 5.75) vs 40-43 (mean 37.8, IQR 7.25), p=0.000042] when the arterial cannula was 16 Fr, 18 Fr, and 20 Fr, respectively. Blue box: IABP. Orange box: K-Beat. IABP, intra-aortic balloon pumping; and IQR, interquartile range.

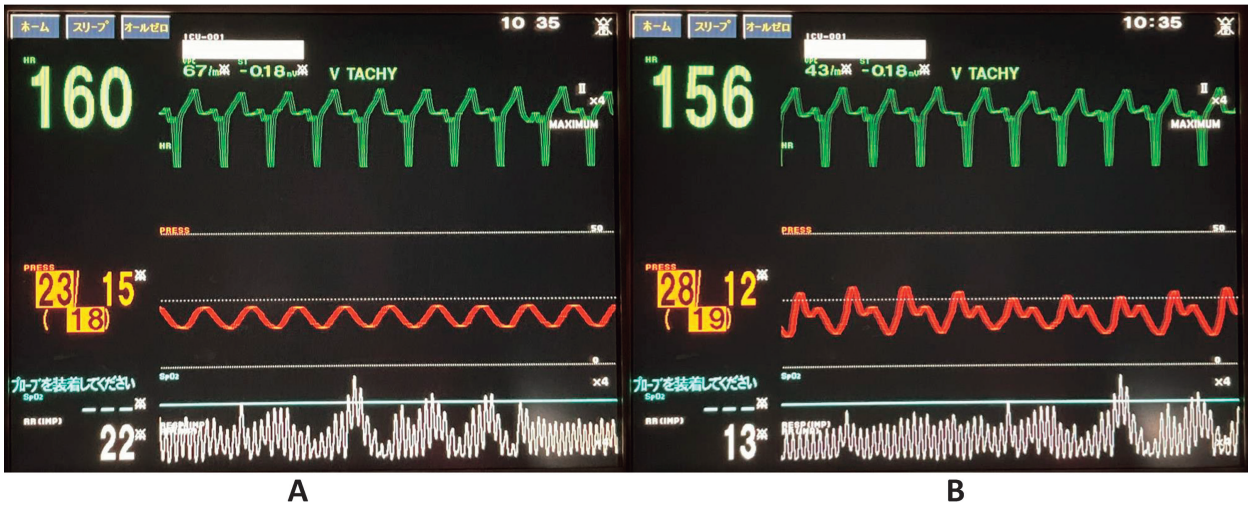

Figures 6. Monitor display.

A. K-Beat off.

B. K-Beat on. The diastolic blood pressure increased, whereas the end-diastolic blood pressure decreased. A heart rate of 160 bpm was recorded and synchronized with the electrocardiogram.

Green line: electrocardiograph. Red line: abdominal aortic pressure.

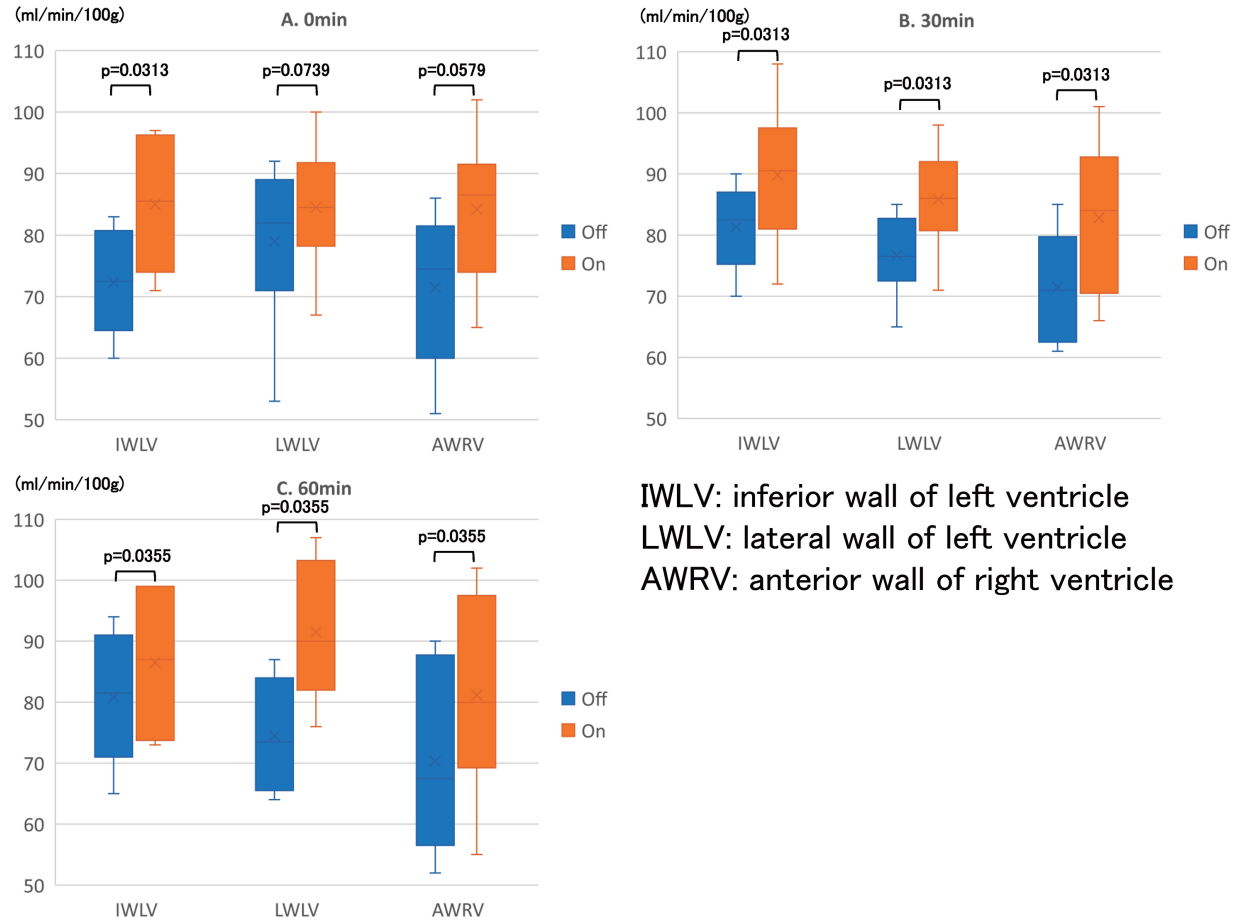

Figures 7. Myocardial perfusion on three cardiac areas.

A. At 0 min, the myocardial perfusion of the IWLV, LWLV, and AWRV was [(mean 71.5, IQR 16.25) vs (mean 85.0, IQR 22.25), p=0.0313]; [(mean 79.0, IQR 18.00) vs (mean 84.5, IQR 13.50), p=0.0739]; and [(mean 71.5, IQR 21.50) vs (mean 84.2, IQR 17.50), p=0.0579], respectively.

B. At 30 min, the myocardial perfusion of the IWLV, LWLV, and AWRV was [(mean 81.3, IQR 11.75) vs (mean 89.8, IQR 16.50), p=0.0313]; [(mean 76.7, IQR 10.25) vs (mean 85.8, IQR 11.25), p=0.0313]; and [(mean 71.5, IQR 17.25) vs (mean 82.8, IQR 22.25), p=0.0313], respectively.

C. At 60 min, the myocardial perfusion of the IWLV, LWLV, and AWRV was [(mean 80.8, IQR 20.00) vs (mean 86.5, IQR 25.25), p=0.0355]; [(mean 74.5, IQR 18.50) vs (mean 91.5, IQR 21.25), p=0.0355]; and [(mean 70.3, IQR 31.25) vs (mean 81.2, IQR 28.25), p=0.0355], respectively.

Blue box: K-Beat off. Orange box: K-Beat on. IWLV, inferior wall of left ventricle; LWLV, lateral wall of left ventricle; AWRV, anterior wall of right ventricle; and IQR, interquartile range.

off (60-83, mean 71.5, IQR 16.25) vs K-Beat on (71-97, mean 85.0, IQR 22.25), p=0.0313]; [K-Beat off (77-92, mean 79.0, IQR 18.00) vs K-Baet on (67-100, mean 84.5, IQR 13.50), p=0.0739]; and [K-Beat off (51-86, mean 71.5, IQR 21.50) vs K-Baet on (65-102, mean 84.2, IQR 17.50), p=0.0579], respectively (Fig. 7A).

At 30 min, the myocardial perfusion for the IWLV, LWLV, and AWRV was [(K-Baet off 70-90, mean 81.3, IQR 11.75) vs K-Baet on (65-94, mean 89.8, IQR 16.50), p=0.0313]; [K-Beat off (65-85, mean 76.7, IQR 10.25) vs K-Beat on (71-98, mean 85.8, IQR 11.25), p=0.0313]; and [K-Baet off (61-85, mean 71.5, IQR 17.25) vs K-Baet on (66-101, mean 82.8, IQR 22.25), p=0.0313], respectively (Fig. 7B).

At 60 min, the myocardial perfusion for the IWLV, LWLV, and AWRV was [K-Baet off (65-94, mean 80.8, IQR 20.00) vs K-Beat on (73-99, mean 86.5, IQR 25.25), p=0.0355]; [K-Beat off (64-87, mean

74.5, IQR 18.50) vs K-Baet on (76-107, mean 91.5, IQR 21.25), p=0.0355]; and [K-Baet off (52-90, mean 70.3, IQR 31.25) vs K-Beat on (55-102, mean 81.2, IQR 28.25), p=0.0355], respectively (Fig. 7C).

Diastolic augmentation by pulsatile flow was consistent with improved coronary perfusion, suggesting the physiological efficacy of K-Beat.

Discussion

K-Beat was as effective as IABP in generating pulsatile flow. In the experiments using a simulated circuit, significant difference was observed when the arterial cannula was 16 Fr and 20 Fr, the K-Beat produced a significantly larger pulse pressure than the IABP. The reason why no significant difference was observed when the arterial cannula was 18 Fr is unknown.

In the animal experiments, the K-Beat was installed in existing pediatric VA-ECMO devices and was used without any problems. Thus, the K-Beat could achieve therapeutic effects equivalent to those of IABP without imposing additional invasive procedures on patients.

Fujii et al[9] reported that they applied VA-ECMO with K-Beat to pigs and observed diastolic augmentation and systolic unloading. Since pigs are large animals, their heart rate was 75-87 bpm, but in this experiment, the system was able to follow the ECG even at 160 bpm. Furthermore, while Fujii et al[9] reported that effective diastolic augmentation was achieved but systolic unloading was not, both diastolic augmentation and systolic unloading were achieved in this experiment. The coronary arteries possess an autoregulating mechanism that adjusts blood flow by increasing microvascular resistance in response to increases in peripheral coronary artery pressure[10]. Compared to when K-Beat was off, there was a significant increase when K-Beat was on, suggesting that K-Beat effectively produced diastolic augmentation.

Three hypotheses can be derived from this animal experiment. The first hypothesis is that diastolic augmentation is easily assumed to be caused by compression of the K-Beat, but systolic unloading was also observed, and the recoil of the pillow is considered to be a possible cause. In this regard, while IABP generates negative pressure by rapidly deflating the balloon, the pillow's recoil in the K-Beat occurs solely due to the pillow's elasticity, leading to reduced hemolysis compared to IABP. Secondly, in this experiment, diastolic augmentation did not exceed systolic blood pressure. One possible reason is that this was an experiment conducted under beating heart conditions, where systolic blood pressure driven by spontaneous cardiac output was dominant. Another reason is that, as described later, the priming volume within the VA ECMO circuit was minimized to the extreme, resulting in the use of a relatively small pillow. If a larger pillow had been used, larger diastolic augmentation and systolic unloading might have been achieved. Furthermore, if a larger diastolic augmentation is achieved, it is possible that better coronary perfusion may be obtained due to autoregulating function of the coronary arteries. Thirdly, the lack of significant differences in LWLV and AWRV between K-Beat on and off immediately after ECMO initiation may be due to the gradual weakening of spontaneous cardiac output over time due to anemia or acidosis, making the effects of the pulsatile flow generated by K-Beat more pronounced. However, no time-dependent decrease in myocardial blood flow was observed in this experiment, so this could not be proven.

In this study, we encountered problems with the progression of anemia. Consequently, we first used existing pediatric systems for the centrifugal pump and oxygenator, which indicated that their volumes could not be further reduced. Therefore, we fully shortened the circuit tubing, reduced the priming volume to 120 mL, and minimized the dilution rate. This volume is considered appropriate

because it was also used for priming in another experiment using rabbits[11], which has indicated the use of 120 mL of blood collected from rabbits as blood donors. Furthermore, from an animal welfare perspective, as in experiments[12-14] where ECMO was applied to rabbits, no rabbits were prepared for blood donation. However, this experiment compared blood flow in the same individual, organ, and site. Moreover, since the rabbits were from the same colony and therefore had the same blood type, the experiment was performed on two rabbits at a time. The ECMO priming for the second rabbit was performed using the blood from the first rabbit. Regarding the sample size, in the previous mouse experiments referenced, n=8[8], and in the rabbit experiments, n=4 and 5[11,12] (both comparisons of two independent groups), therefore, n=6 was considered appropriate, and the experiment was conducted accordingly.

Hemodynamic deterioration occurred >2 h after ECMO initiation, and blood lactate and potassium levels increased sharply. Elevated lactate levels indicate insufficient blood flow, whereas elevated potassium levels suggest hemolysis. Thus, we considered inserting a large-caliber arterial cannula to maintain a low centrifugal pump round rate and ensure a high flow rate. We applied arterial cannulation to the ascending aorta; however, despite performing a purse-string suture, the bleeding was severe, and the rabbit died from blood loss. Therefore, we dissected the neck from the mediastinum to expose the bifurcation of the LCCA and LSCA, ligated the LCCA and LSCA, and cut the bifurcation, enabling the insertion of a large-caliber arterial cannula (14 G catheter) into the BCA. Larsson et al[12] performed laparotomy in rabbits and inserted an 8 Fr arterial cannula into the descending aorta. Additionally, Matsuda et al[14] inserted a 16 G catheter into the BCA and maintained a high flow rate of 70-80 mL/min/kg. However, the ECMO device used in this study was equipped with a roller pump. In a roller pump, the flow rate is proportional to the rotational speed, and the catheter diameter must not be considered. Although roller pumps may be more suitable for maintaining stable hemodynamics over long periods, the experiment was intended to demonstrate the feasibility of installing the K-Beat in existing VA-ECMO devices using centrifugal pumps. Therefore, we could not use this method.

As a limitation, firstly, although we conducted comparative experiments between K-Beat and IABP in the simulated circuit experiment, we did not conduct animal experiments. To prove the superiority of K-Beat, further experiments comparing K-Beat and IABP in animals are necessary. Secondly, the data collected within 1 h were used in this experiment. This was because based on the abovementioned issues, data exceeding 2 h were considered unsuitable for evaluation. Based on numerous experiments applying ECMO to rabbits[12,13,15-19], approximately 4 h is the maximum time required to apply ECMO in rabbits. However, in the experiments by Larsson and Tweddell et al[12,13], roller pumps were used, whereas in the experiments by Brisbois, Yu, Doglass, Bellomo, Griffin et al[15-19], tubes coated with the test coating material were simply used in a common carotid artery-internal jugular vein shunt. Therefore, we were unable to identify the cause of extreme difficulty in continuing to operate the ECMO device for 4 h, and we were unable to use this information as a reference. It is considered necessary to compare the results between the group that underwent extracorporeal circulation with continuous pulsatile flow for a longer duration and the group that underwent extracorporeal circulation with continuous non-pulsatile flow. Thirdly, in this study, we measured myocardial perfusion only under heart beating. Since during cardiac arrest, it is impossible to provide pulsatile flow to the coronary arteries. Therefore, in order to demonstrate the efficacy of incorporating K-Beat into VA-ECMO, it is essential to measure organ perfusion other than heart.

Lastly, the final objective of this experimental system was clinical application in humans. To achieve this, using animals larger than rabbits, generating a pulsatile flow for longer periods under cardiac arrest extracorporeal circulation, and verifying its effects on other organs are necessary.

Acknowledgement

All authors have no COI to declare regarding the present study.

References

1. Spinale FG. The bioactive peptide endothelin causes multiple biologic responses relevant to myocardial and vascular performance after cardiac surgery. J Thorac Cardiovasc Surg 2002;123:1031-1034.
2. Minami K, Körner MM, Vyska K, et al. Effects of pulsatile perfusion on plasma catecholamine levels and hemodynamics during and after cardiac operations with cardiopulmonary bypass. J Thorac Cardiovasc Surg 1990;99:82-91.
3. Landymore RW, Murphy DA, Kinley CE, et al. Does pulsatile flow influence the incidence of postoperative hypertension? Ann Thorac Surg 1979;28:261-268.
4. Hutcheson IR, Griffith TM. Release of endothelium-derived relaxing factor is modulated both by frequency and amplitude of pulsatile flow. Am J Physiol 1991;261:H257-262.
5. Kunst G, Milojevic M, Boer C, et al. 2019 EACTS/EACTA/EBCP guidelines on cardiopulmonary bypass in adult cardiac surgery. Br J Anaesth 2019;123:713-757.
6. Tan A, Newey C, Falter F. Pulsatile perfusion during cardiopulmonary bypass: a literature review. J Extra Corpor Technol 2022;54:50-60.
7. JCS/JSCVS/JCC/CVIT 2023 Guideline Focused Update on Indication and Operation of PCPS/ECMO/IMPELLA. https://www.j-circ.or.jp/cms/wp-content/uploads/2023/03/JCS2023_nishimura.pdf
8. Inamori S, Shirai M, Yahagi N, et al. A comparative study of cerebral microcirculation during pulsatile and nonpulsatile selective cerebral perfusion: assessment by synchrotron radiation microangiography. ASAIO J 2013;59:374-379.
9. Fujii Y, Akamatsu N, Yamasaki Y, et al. Development of a pulsatile flow-generating circulatory assist device (K-Beat) for use with veno-arterial extracorporeal membrane oxygenation in a pig model study. Biology (Basel). 2020;9:121.
10. De Silva K, Lumley M, Kailey B, et al. Coronary and microvascular physiology during intra-aortic balloon counterpulsation. JACC Cardiovasc Interv 2014;7:631-640.
11. Pohlmann JR, Toomasian JM, Hampton CE, et al. The relationship between air exposure, negative pressure, and hemolysis. ASAIO J 2009;55:469-473.
12. Larsson M, Forsman P, Hedenqvist P, et al. Extracorporeal membrane oxygenation improves coagulopathy in an experimental traumatic hemorrhagic model. Eur J Trauma Emerg Surg 2017;43:701-709.
13. Tweddell JS, Khamaf M, Zafar F, et al. Targeting the contrast system in a rabbit model of extracorporeal membrane oxygenation. Blood Adv 2023;7:1404-1417.
14. Matsuda K, Mitsuo H, Nishijima T, et al. Acute dapagliflozin administration ameliorates cardiac surgery-associated acute kidney injury in a rabbit model. Circ J 2024;88:1488-1498.
15. Brisbois EJ, Major TC, Goudie MJ, et al. Improved hemocompatibility of silicone rubber extracorporeal tubing via solvent swelling-impregnation of S-nitroso-N-acetylpenicillamine (SNAP) and evaluation in rabbit thrombogenicity model. Acta Biomater 2016;37:111-119.
16. Yu J, Brisbois E, Handa H, et al. The immobilization of a direct thrombin inhibitor to a polyurethane as a nonthrombogenic surface coating for extracorporeal circulation. J Mater Chem B 2016;4:2264-2272.
17. Douglass ME, Goudie MJ, Pant J, et al. Catalyzed nitric oxide release via Cu nanoparticles leads to an increase in antimicrobial effects and hemocompatibility for short term extracorporeal circulation. ACS Appl Bio Mater 2019;2:2539-2548.
18. Bellomo TR, Jeakle MA, Meyerhoff ME, et al. The effects of the combined argatroban/nitric oxide-releasing polymer on platelet microparticle-induced thrombogenicity in coated extracorporeal circuits. ASAIO J 2021;67:573-582.
19. Griffin L, Douglass M, Goudie M, et al. Improved polymer hemocompatibility for blood-contacting applications via *S*-nitrosoglutathione impregnation. ACS Appl Mater Interfaces 2022;14:11116-11123.

Osaka City Med. J. Vol. 72, 29-38, 2026

Serum Sodium Levels and Their Clinical Associations in Individuals with Severe Motor and Intellectual Disabilities: A Retrospective Study

Tomoyo Yamashita[1,2], Hiroshi Inada[2], Katsuji Tanaka[2,3], and Takashi Hamazaki[1]

Departments of Pediatrics[1] and Donated Course Disability Medicine and Regenerative Medicine[3], Graduate School of Medicine, Osaka Metropolitan University; and Department of Pediatrics[2], Nishinomiya-Sunago Medical and Welfare Center

Abstract

Background

Clinical hyponatremia is frequently observed in individuals with severe motor and intellectual disabilities (SMID) due to disturbances in homeostasis, including water-electrolyte imbalances associated with bedridden status, tube feeding, and chronic polypharmacy. However, no large-scale cross-sectional studies have been conducted to date.

Methods

We conducted a retrospective observational study including individuals with severe motor and intellectual disabilities (SMID) residing in a long-term care facility, using laboratory data collected over the course of one year. This retrospective observational study targets SMID patients who were hospitalized for extended periods. Serum sodium (Na) levels were extracted, and background characteristics, seasonal variations, and associations with laboratory parameters were examined. A representative serum Na value was calculated for each individual, and analyses were performed according to total salt intake, disease severity as classified by the Oshima classification, and carbamazepine (CBZ) use.

Results

A total of 161 were included, with a median age of 54 years; 78 patients (48.4%) were male. Most patients (68.9%) were classified as Oshima category 1. The hyponatremia group consisted of 26 patients (17%). The median representative serum Na level was 140 mEq/L (range: 127-150 mEq/L). Patients in the Oshima category 1 had significantly lower Na levels compared with those in categories ≧2 ($p=0.005$). Hyponatremia was significantly more frequent among CBZ users ($p=0.009$).

Conclusions

In patients with SMID, hyponatremia was associated with Oshima category 1 and with CBZ use, each representing an independent risk factor. These findings offer valuable insights for clinical

Received September 2, 2025; accepted November 25, 2025.
Correspondence to: Tomoyo Yamashita, MD.
Department of Pediatrics, Graduate School of Medicine, Osaka Metropolitan University,
1-4-3 Asahimachi, Abeno-ku, Osaka 545-8585, Japan
Tel: +81-6-6645-3816; Fax: +81-6-6636-8737
E-mail: carina.canopus.1007@gmail.com

practice, particularly for guiding the periodic evaluation and adjustment of medications.

Key Words: Severe motor and intellectual disability; Hyponatremia; Tube feeding; Oshima classification; Serum sodium

Introduction

Severe motor and intellectual disabilities (SMID) are characterized by the coexistence of profound intellectual disability and severe motor impairments. In Japan, the Oshima classification is used to categorize SMID, with categories 1-9 considered representative of the condition; a lower number indicates greater severity[1,2]. The estimated prevalence of SMID is approximately 0.2-0.4 per 1000 people, corresponding to approximately 43000 people nationwide, with numbers rising annually[3,4]. Individuals with SMID frequently experience long-term bedridden status, tube feeding, and chronic polypharmacy, all of which increase the risk of homeostatic disturbances, including water-electrolyte imbalances. Among these, hyponatremia is particularly concerning due to its potential impact on the central nervous system and the difficulty in detecting symptoms in this population.

In individuals with SMID, impaired thirst perception disrupts self-regulation of water intake, and fluid supplementation is typically managed uniformly by caregivers, which may lead to unintended over- or under-administration of fluids. Additional contributing factors include sodium loss through drooling or gastric fluid drainage, abnormal antidiuretic hormone (ADH) secretion due to brain injury, diuretic use, renal dysfunction, and complications such as pneumonia. These factors may precipitate the syndrome of inappropriate antidiuretic hormone secretion (SIADH)[5]. In a previous study of nine patients with SMID with chronic hyponatremia receiving carbamazepine (CBZ), seven were clinically suspected to have SIADH, although elevated ADH levels above the detection threshold were observed in only one patient[6]. These finding suggests that CBZ may contribute to hyponatremia independently of excessive ADH secretion.

The World Health Organization (WHO) recommends limiting salt intake to less than 5g/day in the general adult population[7]. Although the minimum requirement for physiological function is not well defined, the daily sodium requirement is estimated at 200-500 mg (equivalent to 0.5-1.3g of salt)[7]. However, specific target salt intake levels or reference serum sodium (Na) values have been established for individuals with SMID. To the best of our knowledge, no study has investigated whether factors such as seasonality, age, or severity of disability influence serum Na concentrations.

Despite its clinical relevance, the distribution and determinants of serum Na levels in patients with SMID remain poorly characterized. In this retrospective observational study, we examined serum Na concentrations over one year in residential care facilities, identified factors associated with hyponatremia, and aimed to provide clinically useful information for salt supplementation and serum monitoring in this population.

Methods

Study design and participants

This retrospective observational study was conducted at the Sunago Medical Welfare Center in Hyogo, a residential care facility for individuals with SMID. The study population comprised residents who were continuously hospitalized throughout fiscal year 2023 (from April 1, 2023, to March 31, 2024). Exclusion criteria included new admissions or discharges due to death during the study period, cases corresponding to Oshima classification category 10 or higher, and residents

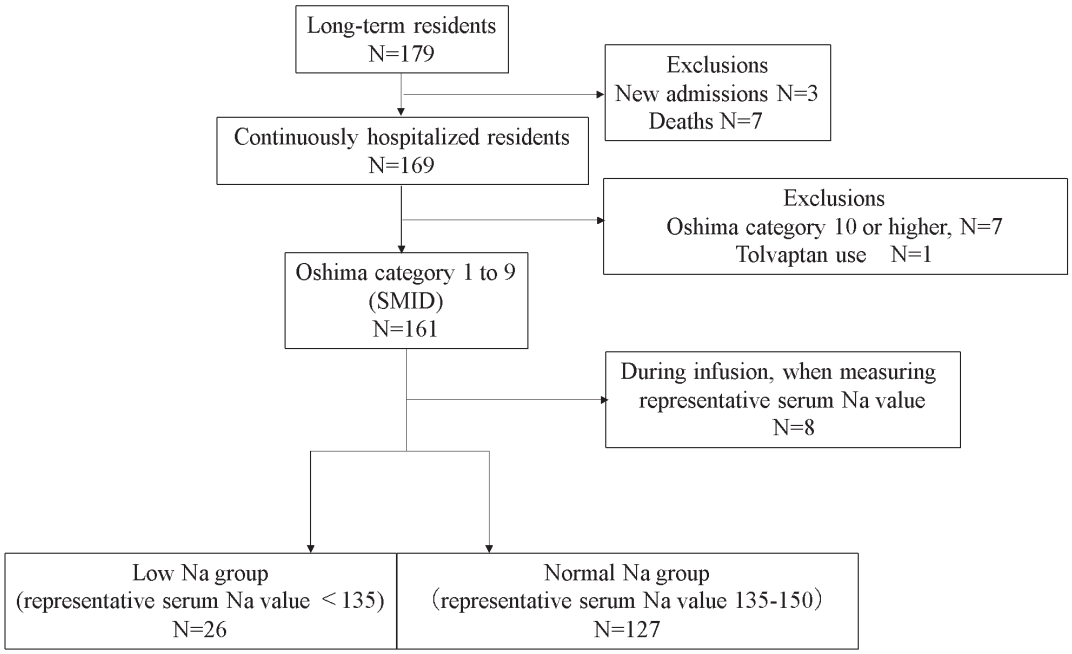

Figure 1. Flow chart.
This is a flow chart showing the inclusion and exclusion criteria for this study.

receiving tolvaptan.

Data collection

The severity of SMID was assessed using the Oshima classification[2]. Participant characteristics, including age, sex, and Oshima classification category, as well as medical interventions such as tube feeding, oral sodium chloride (NaCl) supplementation, and the use of diuretics, CBZ, and tolvaptan, were extracted from medical records. Clinical data included serum Na concentrations measured as part of routine clinical care during the study period, along with simultaneous measurements of C-reactive protein (CRP), albumin, creatinine, potassium, and chloride levels. Measurement timing was categorized by season according to the Japanese calendar: spring (March-May), summer (June-August), autumn (September-November), and winter (December-February).

For each individual, a “representative serum Na value” was defined as the measurement equal to or closest to the median of all serum Na concentrations obtained during the study period. Associations between representative serum Na value and age, sex, and Oshima classification were analyzed.

In addition, correlations were examined between the representative serum Na value and both oral salt intake per body weight and oral sodium chloride supplementation measured on the same day. Participants were further categorized into two groups based on their representative serum Na values: hyponatremia (<135 mEq/L) and normonatremia (135-150 mEq/L). Background factors (sex and severity) and intervention-related factors (tube feeding, dietary salt intake, diuretic use, and CBZ administration) were compared between the two groups. Notably, when analyzing the relationship between representative serum Na and oral salt intake, as well as in the two-group comparisons, cases receiving intravenous infusion at the time of representative serum Na measurement were excluded from the analysis (Fig. 1).

Ethical considerations

This study was conducted in accordance with the principles of the Declaration of Helsinki. All data collection and analyses were performed with strict attention to the protection of personal information. The study protocol was reviewed and approved by the Ethics Committee of Nishinomiya Sunago Medical Welfare Center (approval date: July 14, 2025). Because this was a retrospective study using existing medical records, informed consent was obtained through an opt-out procedure by posting a study notice on the hospital bulletin board. No patients declined participation.

Statistical analysis

Categorical variables are presented as frequencies (N) and percentages (%). For continuous variables, normality was first assessed using the Kolmogorov-Smirnov test. As all variables were non-normally distributed, results are expressed as medians. Seasonal variations in serum Na concentrations were analyzed using one-way analysis of variance (ANOVA) with Bonferroni post hoc tests. Correlations between serum Na and other laboratory parameters, as well as between representative serum Na values and total salt intake, were assessed using Spearman's rank correlation coefficients. Associations between representative serum Na values and sex or SMID severity were examined with the Mann-Whitney U test. Associations between representative serum Na values and medical interventions (Oshima classification, tube feeding, diuretic use, and CBZ use) were examined using logistic regression analysis. Logistic regression analysis was performed using binary comparisons. For the Oshima classification, Category 1 was coded as 0 and Categories 2 and above as 1. For other variables, the absence of a factor was coded as 0 and its presence as 1. To assess multicollinearity, the variance inflation factor (VIF) was calculated. All VIF values were in the range of 1 and below 5, indicating the robustness of the analysis and the absence of multicollinearity. In addition, patients classified as Oshima category 1 are typically bedridden and often require tube feeding, exhibiting markedly different clinical characteristics compared with other classifications. Therefore, analyses were performed separately for Oshima category 1 patients and the remaining patients. All statistical analyses were performed using EZR version 1.54 (Easy R; Saitama Medical Center, Jichi Medical University, Saitama, Japan), a graphical user interface for R (The R Foundation for Statistical Computing, Vienna, Austria), which is a modified version of R Commander version 4.0.3.

Results

A total of 161 participants were included in the study (Fig. 1). Across these participants, 1280 serum Na measurements were collected. Patient characteristics are shown in Table 1. At the end of the observation period (March 31, 2024), the median age was 54 years (range, 12-82 years); 78 participants (48.4%) were male, and 111 (68.9%) were classified as Oshima category 1. The hyponatremia group consisted of 26 patients (17%).

Regarding seasonal variation in serum Na values, the median levels were 137.5 mEq/L in spring, 138.2 mEq/L in summer, 137.2 mEq/L in autumn, and 138.4 mEq/L in winter. In the Bonferroni post-hoc test, the p-values for autumn (which showed the lowest value) compared with spring, summer, and winter were 1.00, 0.06, and 0.014, respectively. A significant difference was observed between the autumn and winter seasons. Correlations between serum Na and other laboratory parameters are presented in Table 2. The only significant correlation was between serum Na and chloride levels (Spearman's $\rho=0.69$, $p<0.0001$).

Table 1. Patient characteristics (N=161)

		median (range) or N (%)
age (y)		54 (12-82)
sex male		78 (48.4%)
body weight (kg)		36.6 (19.4-55.2)
BMI		17 (11-33)
Oshima classification		
	1	111 (68.9%)
	2	29 (18.0%)
	3	4 (2.5%)
	4	3 (1.9%)
	5	11 (6.8%)
	6	2 (1.2%)
	7	0
	8	0
	9	1 (0.6%)
number of serum Na measurements (times)		5 (1-58)
tube feeding		76 (47.2%)
C-reactive protein (mg/dL)		0 (0-9)
albumin (g/dL)		4.1 (2.4-4. 8)
creatinine (mg/dL)		0.52 (0.09-1.54)
potassium (mEq/L)		4.4 (3-5.5)
chloride (mEq/L)		95 (86-111)
oral NaCl supplementation		26 (16.1 %)
	g	3 (1-8.5)
total salt intake (g)		6 (0.9-11.3)
total salt intake per body weight (g/kg)		0.156 (0.029-0.413)
CBZ use		45 (28.0%)
diuretic use		15 (9.3%)
tolvaptan use		1 (0.6%)

BMI, body mass index; NaCl, sodium chloride; and CBZ, Carbamazepine.

Table 2. Correlation between serum Na concentrations and various parameters

	Spearman (ρ)	p values
C-reactive protein	−0.22	<0.001
albumin	0.19	<0.001
creatinine	0.20	<0.001
potassium	−0.07	0.014
chloride	0.69	<0.001

The representative serum Na value was 140 mEq/L (range: 127-150 mEq/L). By Oshima classification, participants in Category 1 had significantly lower representative serum Na values (median 139) compared with those in Category 2 or higher (median 141 mEq/L) (p=0.005) (Fig. 2).

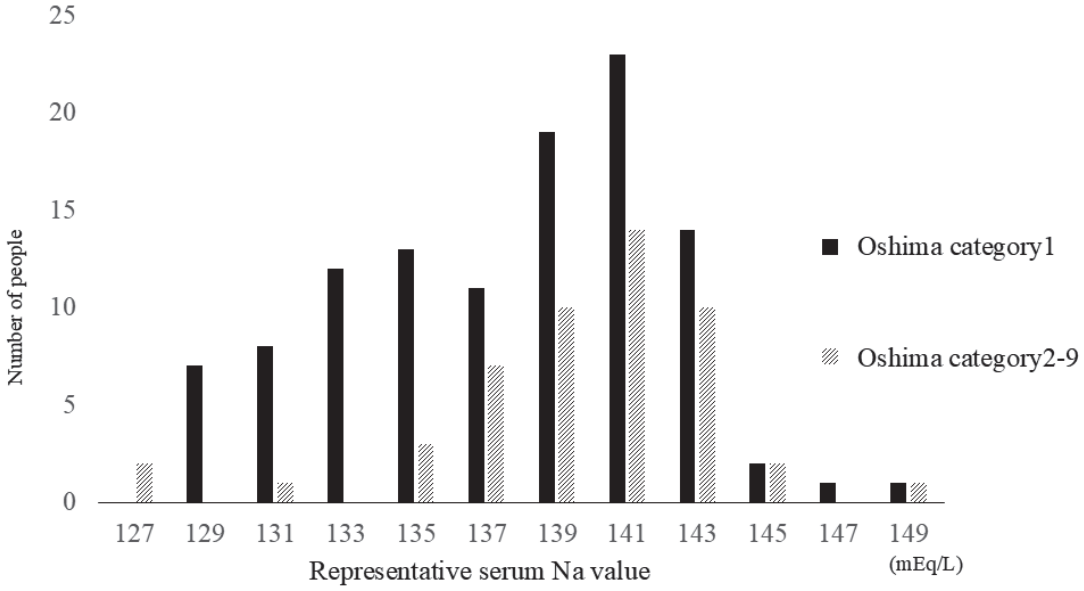

Figure 2. Distribution of representative serum Na levels.
Black indicates the distribution of representative serum sodium levels in Oshima classification category 1, and the dashed line indicates the distribution of representative serum sodium levels in Oshima classification category 2 or higher.

Table 3. Influencing factors in the hyponatremia group

	OR	95%CI	p values
Oshima classification	0.24	(0.06-0.93)	0.039
tube feeding	1.53	(0.58-4.07)	0.39
CBZ use	3.4	(1.35-8.46)	0.009
diuretic use	3.6	(0.93-14)	0.06

OR, Odds ratio; 95% CI, 95% confidence interval; and CBZ, Carbamazepine.

Representative serum Na values were also significantly lower in males (median 139 mEq/L) than in females (median 140 mEq/L) ($p=0.023$). No correlation was observed between representative serum Na values and age (Spearman's $\rho=-0.003$, $p=0.97$).

The median total salt intake (including dietary salt and oral NaCl administered as medication) was 6.0g (range: 0.9-11.3g). When adjusted for body weight, the median total salt intake was 0.152 g/kg (range: 0.029-0.413g). There was no significant correlation between the representative serum sodium level and either the total salt intake or total salt intake per body weight (Spearman's $\rho=-0.02$ and -0.004, with $p=0.8$ and 0.96, respectively).

The results of the analysis of background and intervention factors between the low-Na and normal Na groups are shown in Table 3. A significantly higher proportion of patients with hyponatremia was observed in Oshima Category 1 compared with Categories 2 and above ($p=0.039$). Furthermore, within the hyponatremia group, the proportion of CBZ users was significantly higher than in the normonatremia group ($p=0.009$).

Discussion

Hyponatremia is a frequent complication in patients with SMID; however, no previous study has systematically examined this condition in a large cohort. To the best of our knowledge, this study is

the first to investigate serum Na levels in a large population of >160 patients with SMID and to identify factors associated with hyponatremia. Additionally, among patients with SMID, hyponatremia was significantly more prevalent in those with severe disability classified as Oshima Category 1 and in those receiving CBZ. These findings provide important insights for the clinical management of SMID.

Representative serum Na levels were significantly lower in men (median, 139 mEq/L) than in women (median, 140 mEq/L). Recent studies have reported that the overall average serum Na level for both sexes is approximately 139.4 mmol/L±2 mmol/L, with little difference between men and women[8]. However, a 1990 statistical analysis of serum Na level in healthy American adults reported age-specific, sex-stratified averages: males averaged 139-140 mmol/L, whereas females averaged 138-141 mmol/L, showing a slight tendency toward lower levels in females[9]. The reasons for the lower trend in women are suggested to be differences in body composition, such as muscle mass, and the influence of female hormones[10]. In patients with SMID, previous reports suggest that both males and females have lower levels of sex hormones due to malnutrition and low body weight, leading to delayed puberty onset[11]. Therefore, the influence of sex hormones may be attenuated in female patients with SMID, which could contribute to a reduced likelihood of serum sodium levels decreasing. However, no hormonal analysis was conducted in this study, and further investigation is warranted.

It is well known that serum sodium levels in the elderly exhibit seasonal variation, with the frequency of hyponatremia increasing during the summer. This has been attributed not only to the higher prevalence of renal impairment but also to a decrease in salt intake and an increase in fluid consumption[12]. In this study, unlike previous reports, a difference was observed between autumn and winter. In the residential facility where the participants lived, room temperature was controlled, minimizing the influence of seasonal variation and reducing the likelihood of fluctuations in sweating or fluid balance. Furthermore, the amount of fluid intake in each season was considered appropriate, which may have prevented the occurrence of hyponatremia. As for the relatively lower values observed in autumn, it is possible that the larger temperature fluctuations and summer-like heat during the daytime led to continued fluid supplementation as an extension of summer hydration practices, resulting in slightly higher fluid intake in autumn; however, the details remain unclear. In any case, no clinically meaningful seasonal differences were identified.

In this study, the median daily salt intake among patients with SMID was 6.0g, slightly higher than the WHO-recommended level[7]. By comparison, the reported average daily salt intake for Japanese adults is 11g in men and 9.3g in women, indicating that the intake in our cohort was approximately 60% of the average for Japanese adults[13]. Notably, even with a minimum salt intake of 0.9 g/day, serum Na levels were maintained. According to the Adult and Pediatric Water Balance Study[14], the sodium requirement for maintaining normal balance is estimated at 1-3 mEq/kg (equivalent to 23-69 mg/kg/day), which corresponds to 0.058-0.175 g/kg of salt. In this study, given the characteristic smaller body size of individuals with SMID compared to the general adult population, analyses were conducted based on total salt intake per body weight. The median salt intake was 0.156 g/kg, which falls within this maintenance range; however, individual cases showed intakes both significantly higher and lower than this threshold. An increase in total dietary salt intake does not necessarily lead to a higher representative serum sodium level. This may be explained by physiological mechanisms, such as enhanced renal sodium excretion, concurrent water administration, and hormone-mediated regulation of water balance[15], all of which can attenuate the

direct impact of salt intake on serum sodium levels.

In category 1 of the Oshima classification and category ≧2, the representative Na level was significantly lower in the former (median, 139) than in the latter (median, 141). In older adults, sarcopenia—characterized by reduced muscle mass—has been associated with decreased potassium storage in muscles, resulting in lower total body potassium. This reduction facilitates fluid shifts into the extracellular space, stimulates ADH secretion, and may contribute to hyponatremia[16]. Moreover, hyponatremia is a recognized risk factor for sarcopenia in the elderly[17]. Experimental mouse models indicate that hyponatremia can reduce muscle mass and decrease IGF-1 expression in muscles[18], suggesting a potential bidirectional relationship. From the perspective of activities of daily living, individuals in the Oshima classification category 1 likely have reduced muscle mass compared with those in higher categories, which may predispose them to hyponatremia. Therefore, within the SMID group, Oshima classification category 1 was considered to have a higher risk of developing hyponatremia.

A high prevalence of hyponatremia has been reported among patients on long-term complete enteral nutrition (73 of 175 patients; 42%)[19], and malnourished patients receiving complete enteral nutrition are also considered more likely to develop hyponatremia[20]. Although commercial enteral nutritional formulas contain added salt, their sodium content is intentionally kept relatively low in consideration of patients with hypertension, heart failure, or impaired renal function. In the present study, however, no clear tendency toward hyponatremia was observed among patients receiving enteral nutrition. One possible explanation is that, given the inherently low sodium content of enteral formulas, supplemental oral NaCl had been administered in advance, thereby reducing the likelihood of hyponatremia due to sodium deficiency. Regarding CBZ administration, rat experiments have shown that CBZ increases the sensitivity of vasopressin V2 receptors in renal collecting tubules, enhancing the action of ADH and promoting water reabsorption, thereby causing dilutional hyponatremia[21]. In a study of patients with general epilepsy receiving CBZ, hyponatremia was observed in 17% of those under 40 years of age and in 34% of those 40 years or older, with risk increasing with age[22]. In this study, a significantly higher prevalence of hyponatremia was observed among patients receiving CBZ. Hyponatremia occurred in 2% of CBZ users under 40 years of age and in 28% of those aged 40 years or older, indicating an association between CBZ use and age.

In this study, no significant hyponatremia was observed in patients with SMID who were taking diuretics. This is likely because the diuretics used were either loop or potassium-sparing types, whereas thiazide-type diuretics were not used. Hyponatremia caused by diuretics is most commonly observed with thiazide diuretics, while loop diuretics may cause hyponatremia in cases of fluid overload or extreme fluid intake[23], and potassium-sparing diuretics may lead to hyponatremia when combined with other medications or administered at doses exceeding 100 mg per day[13]. In this study, none of the above conditions were present, and the dosage of potassium-sparing diuretics did not exceed 50 mg/day, suggesting a lower likelihood of developing hyponatremia. One limitation of this study was the absence of a defined target serum Na level for patients with SMID. Consequently, variability existed in the amount of oral NaCl supplementation administered by healthcare providers, which may have acted as a potential confounding factor. Furthermore, since this study was a retrospective observational study, the available data were limited to existing laboratory measurements and medical records, making it difficult to fully adjust for all confounding factors. In the hyponatremia group, detailed evaluations not only of antidiuretic hormone but also of thyroid and adrenal cortical hormones, as well as assessments of urinary sodium excretion, were insufficient.

Further studies with larger sample sizes are warranted to determine the appropriate serum sodium targets for patients with SMID. In conclusion, this study examined serum Na levels in over 160 patients with SMID and identified characteristics associated with a higher risk of developing hyponatremia. Among these patients, those classified as severe according to the Oshima classification (Category 1) and those receiving CBZ were found to be more prone to developing hyponatremia. These findings highlight the importance of establishing target serum Na levels for patients with SMID to guide regular monitoring and optimize medication management, thereby reducing the risk of hyponatremia and its associated complications.

Acknowledgements

All authors have no COI to declare regarding the present study.

We appreciate all members for their contributions. TY was responsible for the overall study, including the design of the study protocol, data analysis, and manuscript writing. HI was responsible for designing the study protocol and data analysis. KT and TH reviewed and revised the manuscript. We want to thank Editage for English language editing.

Reference

1. Taniguchi K, Kamino K, Kudo T, et al. Evaluation of antiepileptic for behavioral symptoms in severe intellectual disabilities. Austin Journal of Psychiatry and Behavioral Sciences 2014;1:1019.
2. Oshima K. Basic issue on severe motor and intellectual disabilities. Kosyu Eisei 1971;35:648-655. (In Japanese)
3. Okada Y. Today's significance of the world's only medical welfare for children with severe motor and intellectual disabilities. Journal of Intellectual & Developmental Disability 2013;38:3-9.
4. Wakimizu R, Fujioka H. Social support needs of caregivers rearing children with severe motor and intellectual disabilities at home in Japan. Front Rehabil Sci 2024;5:1280278.
5. Yagi M. Denkaishitsuijou. Japanese Journal of Pediatric Medicine 2015;47:2095-2097. (In Japanese)
6. Katori S, Nagae A, Fujita Y, et al. The hormone secretion, water and electrolyte balance in nine patients with severe motor and intellectual disabilities with chronic hyponatremia. Journal of Severe Motor and Intellectual Disabilities 2013;38:101-105.
7. World Health Organization. Guideline: Sodium Intake for Adults and Children. Geneva, Switzerland: World Health Organization; 2012. Accessed August 19, 2025. https://www.who.int/publications/i/item/9789241504836.
8. Tong X, Wang F, Liu M. Serum sodium within the normal range and its U-shaped relationship with biological aging in U.S. adults. Front Nutr 2025;12:1589962.
9. Institute of Medicine. Dietary Reference Intakes for Water, Potassium, Sodium, Chloride, and Sulfate. Washington, DC: The National Academies Press; 2005.
10. Vogel AS, Li M, Zucker SD. Aldosterone antagonist dosing and the risk of hyponatremia in patients with cirrhosis and ascites. Gastro Hep Adv 2022;2:2-4.
11. Calcaterra V, Cena H, De Silvestri A, et al. Disorders of puberty in severely neurologically impaired children: is delayed puberty an underestimated problem? Front Pediatr 2019;7:462.
12. Giordano M, Ciarambino T, Castellino P, et al. Seasonal variations of hyponatremia in the emergency department: age-related changes. Am J Emerg Med 2017;35:749-752.
13. Ministry of Health, Labour and Welfare. The national health and nutrition survey in Japan, 2018. Tokyo: Ministry of Health, Labour and Welfare; 2019. Accessed August 19, 2025. https://www.mhlw.go.jp/content/001066884.pdf
14. EFSA Panel on Nutrition, Novel Foods, and Food Allergens (NDA); Turck D, Castenmiller J, de Henauw S, et al. Dietary reference values for sodium. EFSA J 2019;17:e05778.
15. Rakova N, Kitada K, Lerchl K, et al. Increased salt consumption induces body water conservation and decreases fluid intake. J Clin Invest 2017;127:1932-1943.
16. Bertini V, Nicoletti C, Beker BM, et al. Sarcopenia as a potential cause of chronic hyponatremia in the elderly. Med Hypotheses 2019;127:46-48.
17. Karakousis ND, Kostakopoulos NA. Hyponatremia in the frail. J Frailty Sarcopenia Falls 2021;6:241-245.

18. Kawao N, Nishikawa A, Matsumura D, et al. Roles of insulin-like growth factor-1 in muscle wasting and osteopenia in mice with hyponatremia. Calcif Tissue Int 2025;116:61.
19. Kajihara Y. The prevalence and relevant factors of hyponatremia under long-term total enteral nutrition: a cross-sectional study. J Gen Fam Med 2017;18:182-183.
20. Serrano Valles C, Gómez Hoyos E, Ortolá Buigues A, et al. Hyponatremia among patients with total enteral tube feeding: prevalence and associated clinical factors. Nutr Hosp 2022;39:723-727. (In Spanish)
21. de Bragança AC, Moyses ZP, Magaldi AJ. Carbamazepine can induce kidney water absorption by increasing aquaporin 2 expression. Nephrol Dial Transplant 2010;25:3840-3845.
22. Berghuis B, Hulst J, Sonsma A, et al. Symptomatology of carbamazepine- and oxcarbazepine-induced hyponatremia in people with epilepsy. Epilepsia 2021;62:778-784.
23. Jha VK, Padmaprakash KV, Pandey R. Diuretic-induced dyselectrolytemia and its clinical implications. Curr Med Issues 2019;17:69-74.

Osaka City Med. J. Vol. 72, 39-48, 2026

Association of Nutritional Status Evaluated by the Geriatric Nutritional Risk Index with Aortic Calcification Score in Patients Undergoing Hemodialysis

Katsuhiro Ono[1,2], Hideki Uedono[1], Katsuhito Mori[3], Shinya Nakatani[1], Akihiro Tsuda[1], Masafumi Kurajoh[1], Shigeichi Shoji[2], Tetsuo Shoji[1], Tomoaki Morioka[1], Tomoyuki Yamakawa[2], and Masanori Emoto[1,3]

Departments of Metabolism, Endocrinology and Molecular Medicine[1] and Nephrology[3], Graduate School of Medicine, Osaka Metropolitan University; and Department of Internal Medicine[2], Kidney Center, Shirasagi Hospital

Abstract

Background

Nutritional disorders are strongly linked to adverse clinical outcomes, including cardiovascular disease (CVD), in patients undergoing hemodialysis. The geriatric nutritional risk index (GNRI) is an objective screening tool for nutritional status that predicts all-cause and CVD mortality. Vascular calcification, a hallmark in this population, is also associated with poor prognosis. However, little is known about the association between nutritional disorders and vascular calcification. Thus, the aim of this study is to examine the association of GNRI with aortic calcification in patients undergoing hemodialysis.

Methods

A cross-sectional study was performed in patients undergoing hemodialysis. The aortic calcification score was quantified using multi-slice computed tomography based on the Agatston score. The potential association between GNRI and aortic calcification score was examined using Spearman rank correlation and multiple regression analysis.

Results

The 374 patients had a median age of 72 years, a median GNRI of 91.5, and a median aortic calcification score of 7836. There was an inverse correlation between GNRI and aortic calcification score ($\rho = -0.143$, $p = 0.006$). In multiple regression analysis, GNRI was independently and inversely associated with aortic calcification score ($\beta = -0.145$, $p = 0.009$) after adjustment for known risk factors.

Conclusions

Lower GNRI was significantly associated with higher aortic calcification in patients undergoing hemodialysis, suggesting a potential link between poor nutritional status and vascular calcification.

Received September 1, 2025; accepted November 25, 2025.
Correspondence to: Hideki Uedono, MD, PhD.
Department of Metabolism, Endocrinology and Molecular Medicine, Graduate School of Medicine, Osaka Metropolitan University, 1-4-3 Asahimachi, Abeno-ku, Osaka 545-8585, Japan
Tel: +81-6-6645-3806; Fax: +81-6-6645-3808
E-mail: uedono1217@omu.ac.jp

Key Words: Aortic calcification; Cardiovascular disease; Geriatric nutritional risk index (GNRI); Hemodialysis

Introduction

The nutritional disorder known as protein-energy wasting (PEW) is common in patients with advanced chronic kidney disease (CKD), especially in those undergoing hemodialysis[1]. PEW is characterized by loss of muscle mass and fuel reserves, and is strongly linked to adverse outcomes[2]. The geriatric nutritional risk index (GNRI), which is calculated based on serum albumin and body mass index, has been proposed as a simple and objective screening tool for nutritional status in patients undergoing hemodialysis[3]. A lower GNRI is significantly associated with higher risks of all-cause mortality[4-6], cardiovascular disease (CVD) mortality[7] , and infection-related mortality[8] in these. A recent meta-analysis showed the usefulness of GNRI as a predictor of mortality in this population[9].

Vascular calcification, a hallmark of advanced CKD, is associated with all-cause and CVD mortality[10,11]. In addition to the burden of traditional risk factors such as diabetes and atherosclerotic disease, non-traditional risk factors are thought to accelerate vascular calcification during development of CVD[12]. Given the close relationship between PEW and CVD, nutritional disorder may be involved in formation of vascular calcification, but this relationship has not been widely studied. An inverse association of GNRI with the semiquantitative severity of aortic calcification has been shown in 323 patients with CKD without dialysis therapy[13]. Another study showed that poor nutrition evaluated by modified subjective global assessment was independently associated with coronary artery calcification in 131 patients undergoing hemodialysis[14]. However, to our knowledge, there has been no study of the association of nutritional status with quantitative aortic calcification based on the Agatston score in patients undergoing hemodialysis. Therefore, to investigate this association, we evaluated GNRI and the aortic calcification score quantified using the Agatston score from multi-slice computed tomography.

Methods

Participants

An observational study was conducted at Shirasagi Hospital, Osaka, Japan. All participants underwent abdominal Computed Tomography (CT) between December 2022 and September 2023. Demographic and anthropometric data were obtained from medical records. Routine laboratory data were measured using blood samples taken from an arteriovenous fistula before hemodialysis sessions with a 2-day interval (Monday or Tuesday).

Hypertension was defined as systolic blood pressure ≧140 mm Hg, diastolic blood pressure ≧90 mm Hg and/or use of any antihypertensive medication[15]. The diagnosis of diabetes mellitus (DM) was based on a history of DM and/or use of anti-hyperglycemic medication and/or the American Diabetes Association criteria[16]. Dyslipidemia was defined as high-density cholesterol (HDL-C) ≦40 mg/dL, non-HDL-C ≧150 mg/dL and/or use of statins[17]. History of CVD events was defined as a past occurrence of ischemic heart disease, stroke, peripheral arterial disease, heart failure, or cardiac valvular disease[18].

The study adhered to the principles of the Declaration of Helsinki. The study protocol was approved by the Ethics Committee of Shirasagi Hospital (JCR2022009). Due to the retrospective observational study, informed consent was obtained using the opt-out method.

Geriatric Nutritional Risk Index (GNRI)

The GNRI was calculated from serum albumin and body weight as follows (4-8): GNRI [14.89× serum albumin (g/dL)]+[41.7×(body weight (kg)/ideal body weight (kg))], where body weight (BW) (kg) refers to the "dry weight" of each participant. If BW/ideal BW (IBW) was ≧1, the value was taken to be 1. IBW was calculated as height $(m)^2 \times 22$[19]

Measurement of aortic calcification

Aortic calcification was evaluated as previously described in our study[20], using the original method developed by Agaston et al[21]. Briefly, 80-slice CT (Aquilion PRIME, Canon Medical Systems, Tochigi, Japan) was used to obtain images with a 0.8 mm slice thickness. Calcification was quantified using calcification measurement software based on the Agatston score on an image analysis workstation (Ziostation 2, Ziosoft Corp., Tokyo, Japan). The measurement range was from one slice above the complete iliac artery bifurcation up to 100 mm. Aortic calcification was defined as the volume of two adjacent pixels with CT density >130 Hounsfield units within the aortic area[20].

Statistical analysis

Continuous and categorical variables are expressed as median [Interquartile range (IQR)] and numbers (%), respectively. Unadjusted correlations of various parameters with the aortic calcification score were examined by Spearman rank correlation. Continuous variables were compared by Mann-Whitney U test, and categorical variables by χ^2 test. Multiple regression analysis was performed to examine whether GNRI was independently associated with aortic calcification score. Clinically important variables, including age, sex, dialysis vintage, diabetes, serum phosphorus, and C-reactive protein (CRP), were included as covariates, as these are known to be associated with vascular calcification. The distributions of CRP levels and aortic calcification scores were skewed, and thus, CRP was logarithmically transformed and the calcification score was square root transformed. Effect modification by classical atherosclerosis-related factors was examined, and stratified analyses were conducted when an interaction was suggested.

All statistical analyses were performed with EZR[22] (ver.1.63) (Saitama Medical Center, Jichi Medical University, Saitama, Japan). EZR is a graphical user interface for R (The R Foundation for Statistical Computing, Vienna, Austria) that is a modified version of R commander with statistical functions frequently used in biostatistics. The level of significance was set at $p < 0.05$.

Results

The participant selection process is shown in Figure 1. Of 389 patients initially recruited, 15 were excluded due to a history of aortic surgery (n=10) or the presence of aortic dissection (n=3) or aortic aneurysm (n=2) because these conditions may affect the calcification score. This left a total of 374 participants for analysis (Table 1). The median [IQR] age was 72 [61-79] years and 246 participants (65.8%) were male.

Of the 374 participants, 165 (44.1%) had diabetes, 324 (86.6%) had hypertension, 213 (57.0%) had dyslipidemia, and 199 (53.2%) had a history of cardiovascular events.

The median GNRI and aortic calcification score were 91.5 [86.1-95.3] and 7836 [3279-12941], respectively. Representative measurements of aortic calcification were shown in Figure 2. The distribution of GNRI and aortic calcification score was shown (Figs. 3a and 3b) and the aortic calcification score was square-root transformed (Fig. 3c). Spearman rank correlation analysis revealed an inverse correlation of aortic calcification score with GNRI ($\rho = -0.143$, $p = 0.006$), as well

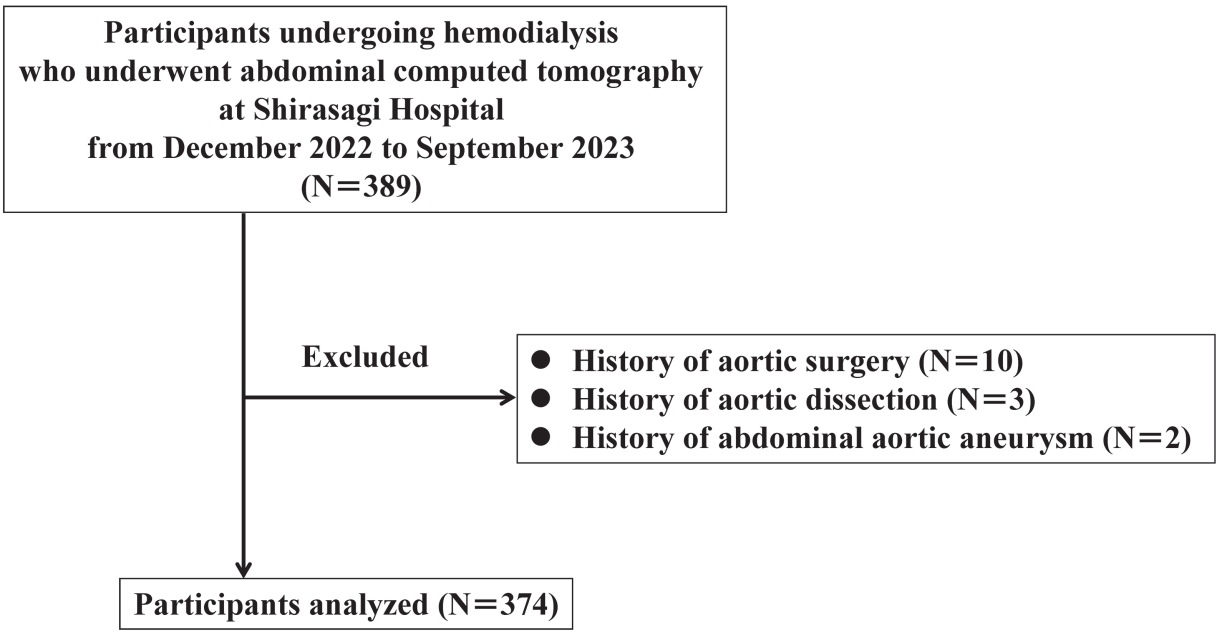

Figure 1. Flow diagram showing the disposition of patients in the study.

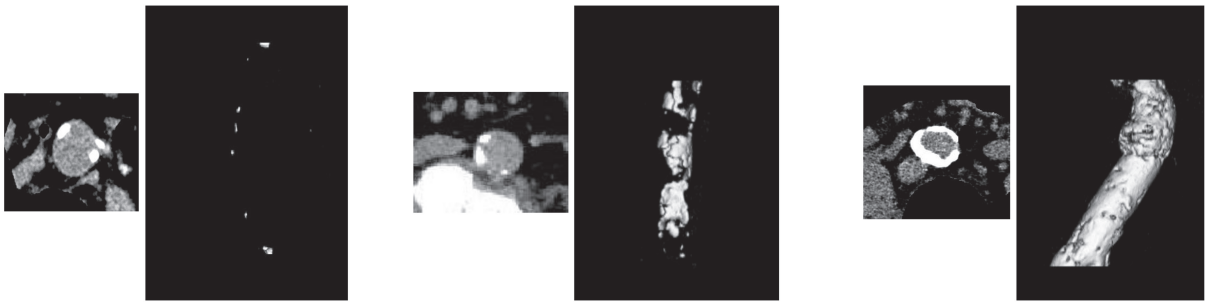

Figure 2. Representative computed tomography images used to calculate the aortic calcification score based on the Agatston method.

as with serum creatinine, age, and serum magnesium (Table 2, Figs. 4a-4d). Conversely, age exhibited a strong positive correlation with aortic calcification score ($\rho=0.305$, $p<0.001$).

In multiple regression analysis, GNRI had a significant independent association with aortic calcification score ($\beta=-0.145$, $p=0.009$). In the same model, serum phosphate ($\beta=0.025$, $p=0.611$) and serum magnesium ($\beta=0.028$, $p=0.565$) were not significantly associated with aortic calcification score (Table 3).

We explored whether the association between GNRI and aortic calcification score was modified by classical atherosclerosis-related factors. Although no significant interactions were observed for hypertension, dyslipidemia, or smoking, a possible effect modification by diabetes was suggested (P for interaction=0.114). Therefore, we stratified the analysis by diabetes status. The aortic calcification score was significantly higher in patients with diabetes than in those without

Table 1. Clinical characteristics

	All (n=374)
Age (years)	72 [61-79]
Male/female (N, %)	246/128 (65.8 / 34.2)
Duration of hemodialysis (years)	9.9 [7.6-15.0]
Diabetes (%)	165 (44.1)
Hypertension (%)	324 (86.6)
Dyslipidemia (%)	213 (57.0)
Current smoking (%)	53 (14.2)
History of cardiovascular disease (%)	199 (53.2)
Body mass index (kg/m^2)	21.8 [19.3-24.5]
Serum albumin (g/dL)	3.5 [3.3-3.7]
Serum creatinine (mg/dL)	9.5 [8.1-11.4]
C-reactive protein (mg/dL)	0.2 [0.1-0.7]
Calcium (mg/dL)	8.6 [8.1-9.0]
Phosphorus (mg/dL)	4.7 [3.9-5.5]
Magnesium (mg/dL)	2.3 [2.1-2.6]
Intact parathyroid hormone (pg/mL)	146 [91-212]
Geriatric Nutritional Risk Index	91.5 [86.1-95.3]
Aortic calcification score	7836 [3279-12941]

Data are expressed as numbers (percentages) or median [interquartile range].

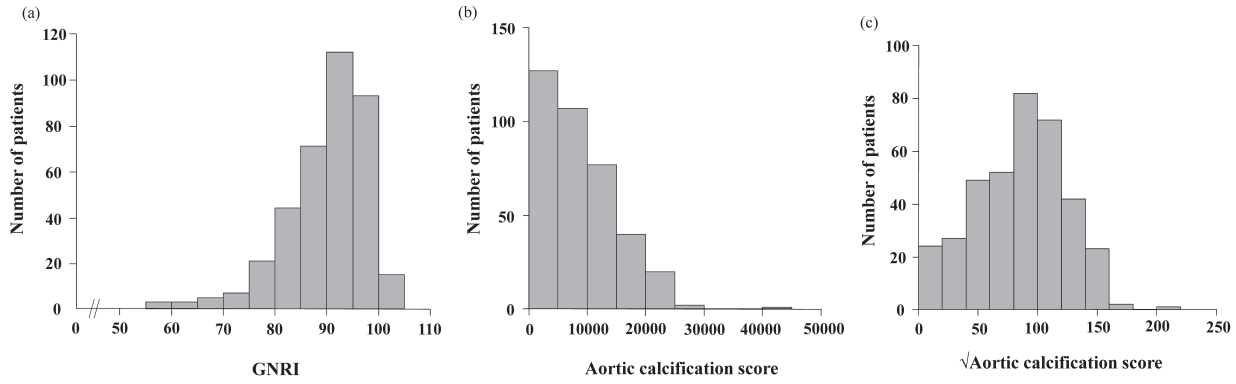

Figure 3. Histograms showing the distributions of the Geriatric Nutritional Risk Index (GNRI) and aortic calcification score, along with their square root-transformed counterparts. The square root-transformed aortic calcification score was expressed as √Aortic calcification score. The median GNRI and aortic calcification score were 91.5 [86.1-95.3] and 7836 [3279-12941], respectively.

(8421 vs 6904, p=0.008) (Fig. 5). In patients without diabetes, the results of multiple regression analysis were consistent with the main analysis, while no significant association between GNRI and aortic calcification score was observed in the diabetic subgroup (Table 4).

Discussion

In this cross-sectional study, we found that lower GNRI was significantly associated with higher aortic calcification quantified by multi-slice CT in patients undergoing hemodialysis. Spearman's rank correlation revealed a significant inverse association between GNRI and aortic calcification score ($\rho=-0.143$, p=0.006), and this relationship remained significant in multivariable regression

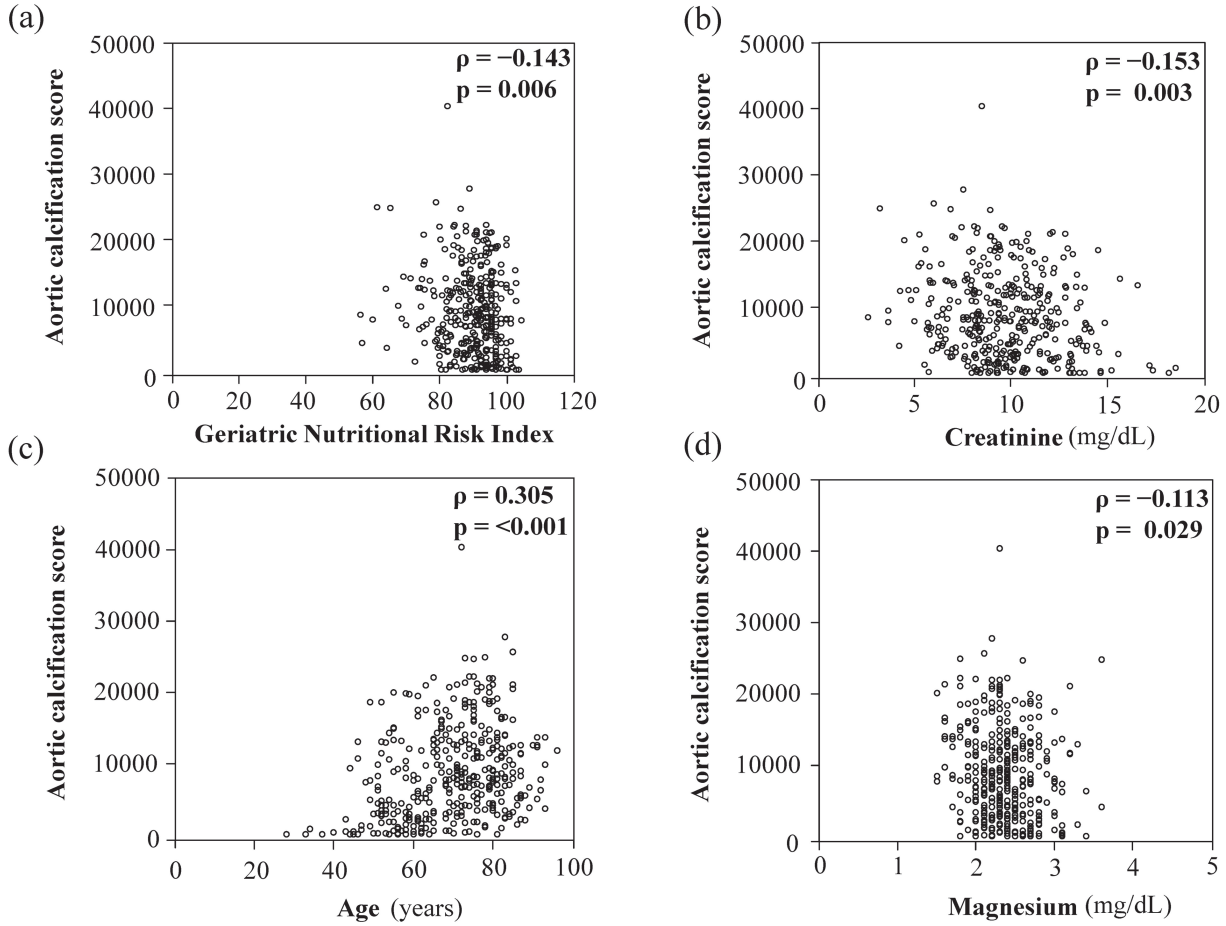

Figure 4. Spearman's rank correlation revealed an inverse correlation of aortic calcification score with geriatric nutritional risk index (GNRI) (ρ=−0.143, p=0.006), as well as age, serum creatinine, and serum magnesium.

Table 2. Correlations of clinical factors with aortic calcification score

	ρ	p
Age	0.305	<0.001
Duration of hemodialysis	0.069	0.184
Body mass index	−0.082	0.113
Serum albumin	−0.161	0.002
Serum creatinine	−0.153	0.003
C-reactive protein	0.003	0.955
Serum calcium	0.047	0.366
Serum phosphorus	−0.017	0.738
Serum magnesium	−0.113	0.029
Intact parathyroid hormone	0.011	0.832
Geriatric Nutritional Risk Index	−0.143	0.006

ρ, Spearman rank correlation coefficient.

analysis (β=−0.145, p=0.009).

Harada et al reported an inverse association between GNRI and the semi-quantitative aortic calcification index (ACI) in non-dialyzed patients with CKD[13], and Huang et al found that poor nutrition evaluated by modified subjective global assessment was associated with coronary artery

Table 3. Multiple regression analysis of the association of clinical factors with aortic calcification score

	β	p
Age	0.423	<0.001
Sex (male=1, female=0)	0.175	<0.001
Duration of hemodialysis	0.090	0.054
Diabetes mellitus (presence=1, absence=0)	0.118	0.016
Hypertension (presence=1, absence=0)	0.117	0.011
Dyslipidemia (presence=1, absence=0)	0.048	0.294
Current smoking (presence=1, absence=0)	0.172	<0.001
History of cardiovascular disease (presence=1, absence=0)	0.247	<0.001
Serum creatinine	0.036	0.576
Log C-reactive protein	−0.029	0.543
Serum calcium	0.090	0.053
Serum phosphorus	0.025	0.611
Serum magnesium	0.028	0.565
Intact parathyroid hormone	0.028	0.532
Geriatric Nutritional Risk Index	−0.145	0.009
Adjusted R^2/p	0.31/<0.001	

β, standard regression coefficient by multiple regression analysis; and R^2, multiple coefficients of determination.

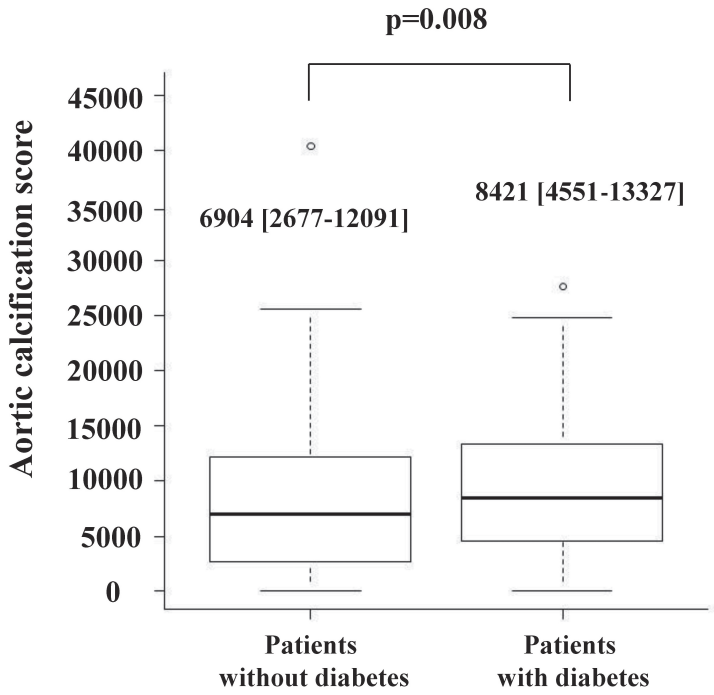

Figure 5. Comparison of aortic calcification scores between patients with and without diabetes. Patients with diabetes had significantly higher scores than those without diabetes (median, 8421 vs 6904; p=0.008).

calcification in patients undergoing hemodialysis[14]. In a retrospective longitudinal observational study to examine whether GNRI could predict changes in ACI in patients undergoing hemodialysis, Okamoto et al[23] showed that low GNRI was an independent risk factor for progression of aortic calcification, suggesting that poor nutrition could exacerbate vascular calcification. The current study showed an association between GNRI and abdominal aortic calcification assessed by the Agatston

Table 4. Multiple regression analysis of associations of clinical factors with aortic calcification score in patients with or without diabetes

	Without diabetes (N=209)		With diabetes (N=165)	
	β	p	β	p
Age	0.492	<0.001	0.293	0.002
Sex (male=1, female=0)	0.149	0.019	0.195	0.012
Duration of hemodialysis	0.091	0.141	0.047	0.513
Hypertension (presence=1, absence=0)	0.126	0.039	0.109	0.137
Dyslipidemia (presence=1, absence=0)	0.054	0.370	0.007	0.923
Current smoking (presence=1, absence=0)	0.235	<0.001	0.084	0.264
History of cardiovascular disease (presence=1, absence=0)	0.179	0.003	0.336	<0.001
Serum creatinine	0.038	0.660	0.056	0.588
Log C-reactive protein	0.011	0.857	−0.027	0.737
Serum calcium	0.118	0.059	0.041	0.580
Serum phosphorus	−0.002	0.972	0.064	0.435
Serum magnesium	0.056	0.382	−0.032	0.692
Intact parathyroid hormone	0.026	0.543	0.017	0.812
Geriatric Nutritional Risk Index	−0.192	0.007	−0.135	0.164
Adjusted R^2/p	0.34/<0.001		0.23/<0.001	

β, standard regression coefficient by multiple regression analysis; and R^2, multiple coefficients of determination.

score in patients undergoing hemodialysis. These findings suggest that GNRI is a clinically useful marker reflecting the severity of vascular calcification and may contribute to assessment of calcification risk in patients undergoing hemodialysis.

The underlying mechanisms linking poor nutritional status and vascular calcification are uncertain, but the mechanism may originate from low protein intake. Both low and high protein intakes are detrimental in patients undergoing hemodialysis[24,25]. Low protein intake may exacerbate PEW, resulting in a higher risk of cardiovascular death and all-cause mortality. In adenine-induced uremic rats, a low protein diet exacerbated arterial medial calcification without changes in phosphate, parathyroid hormone, and creatinine[26]. Furthermore, restriction of dietary protein has been found to promote vascular calcification by lowering fetuin-A, a well-known calcification inhibitor, in uremic rats[27]. Fetuin-A, a predictor for CVD events in hemodialysis patients[28], is strongly induced by nutritional factors such as glucose and fatty acids[29]. Indeed, GNRI and fetuin-A showed a significant interaction in prediction of CVD events in 388 patients undergoing hemodialysis, although vascular calcification was not examined[30]. A low fetuin-A level was associated with more cardiovascular events in patients with poor nutritional status[31], which may reflect the contribution of vascular calcification. Poor dietary intake may also lead to a deficiency of other calcification inhibitors, such as albumin, magnesium, and zinc, resulting in acceleration of vascular calcification[31]. Conversely, vascular calcification may contribute to nutritional disorders since it decreases blood flow and organ perfusion[32], and an impaired supply of oxygen and nutrients to various organs could lead to PEW. Further studies are needed to examine the possible vicious cycle between nutritional disorders and vascular calcification.

Notably, neither serum phosphate nor serum magnesium levels showed a significant association with the aortic calcification score in our study. This may partly be explained by the use of phosphate binders in about 70% of the patients, as well as concomitant use of magnesium oxide preparations in

some patients, both of which could have influenced serum levels.

Intriguingly, there was also no significant association between GNRI and aortic calcification score in patients with diabetes. Diabetes, along with aging and CKD, is recognized as a major contributory factor to development of vascular calcification. Indeed, previous studies have reported that the progression of coronary artery calcification is more rapid in patients with diabetes than in those without diabetes[33]. Therefore, the presence of diabetes may have accelerated vascular calcification prior to initiation of dialysis.

This study has several limitations. First, due to its cross-sectional design, causality cannot be inferred. Second, we did not compare GNRI with other nutritional screening tools. Third, we did not measure fetuin-A and zinc levels, which are known to be associated with vascular calcification. Finally, the study was conducted at a single center with a relatively small sample size.

In conclusion, poorer nutritional status evaluated by GNRI was significantly associated with higher aortic calcification in patients undergoing hemodialysis. Nutrition deterioration may be related to the progression of vascular calcification, suggesting the importance of nutritional assessment in patients undergoing hemodialysis.

Acknowledgements

All authors have no COI to declare regarding the present study.

References

1. Fouque D, Kalantar-Zadeh K, Kopple J, et al. A proposed nomenclature and diagnostic criteria for protein-energy wasting in acute and chronic kidney disease. Kidney Int 2008;73:391-398.
2. Ikizler TA, Cano NJ, Franch H, et al. Prevention and treatment of protein energy wasting in chronic kidney disease patients: a consensus statement by the International Society of Renal Nutrition and Metabolism. Kidney Int 2013;84:1096-1107.
3. Yamada K, Furuya R, Takita T, et al. Simplified nutritional screening tools for patients on maintenance hemodialysis. Am J Clin Nutr 2008;87:106-113.
4. Kobayashi I, Ishimura E, Kato Y, et al. Geriatric Nutritional Risk Index, a simplified nutritional screening index, is a significant predictor of mortality in chronic dialysis patients. Nephrol Dial Transplant 2010;25: 3361-3365.
5. Yamada S, Yamamoto S, Fukuma S, et al. Geriatric nutritional risk index (GNRI) and creatinine index equally predict the risk of mortality in hemodialysis patients: J-DOPPS. Sci Rep 2020;10:5756.
6. Machiba Y, Mori K, Shoji T, et al. Nutritional disorder evaluated by the geriatric nutritional risk index predicts death after hospitalization for Infection in patients undergoing maintenance hemodialysis. J Ren Nutr 2022; 32:751-757.
7. Takahashi H, Ito Y, Ishii H, et al. Geriatric nutritional risk index accurately predicts cardiovascular mortality in incident hemodialysis patients. J Cardiol 2014;64:32-36.
8. Matsukuma Y, Tanaka S, Taniguchi M, et al. Association of geriatric nutritional risk index with infection-related mortality in patients undergoing hemodialysis: The Q-Cohort Study. Clin Nutr 2019;38:279-287.
9. Xiong J, Wang M, Zhang Y, et al. Association of geriatric nutritional risk index with mortality in hemodialysis patients: a meta-analysis of cohort studies. Kidney Blood Press Res 2018;43:1878-1889.
10. Okuno S, Ishimura E, Kitatani K, et al. Presence of abdominal aortic calcification is significantly associated with all-cause and cardiovascular mortality in maintenance hemodialysis patients. Am J Kidney Dis 2007;49: 417-425.
11. Schlieper G, Schurgers L, Brandenburg V, et al. Vascular calcification in chronic kidney disease: an update. Nephrol Dial Transplant 2016;31:31-39.
12. Wanner C, Amann K, Shoji T. The heart and vascular system in dialysis. Lancet 2016;388:276-284.
13. Harada K, Suzuki S, Ishii H, et al. Nutrition status predicts severity of vascular calcification in non-dialyzed chronic kidney disease. Circ J 2017;81:316-321.
14. Huang Y, Ge Y, Li F, et al. Elucidating the relationship between nutrition indices and coronary artery

calcification in patients undergoing maintenance hemodialysis. Ther Apher Dial 2022;26:71-84.
15. Umemura S, Arima H, Arima S, et al. The Japanese Society of Hypertension guidelines for the management of hypertension (JSH 2019). Hypertens Res 2019;42:1235-1481.
16. American Diabetes Association. Diagnosis and classification of diabetes mellitus. Diabetes Care 2004;27:S5-S10.
17. Okamura T, Tsukamoto K, Arai H, et al. Japan Atherosclerosis Society (JAS) guidelines for prevention of atherosclerotic cardiovascular diseases 2022. J Atheroscler Thromb 2024;31:641-853.
18. Shah S, Weinhandl E, Gupta N, et al. Cardiovascular outcomes in patients on home hemodialysis and peritoneal dialysis. Kidney360 2024;5:205-215.
19. Tokunaga K, Matsuzawa Y, Kotani K, et al. Ideal body weight estimated from the body mass index with the lowest morbidity. Int J Obes 1991;15:1-5.
20. Ichii M, Ishimura E, Shima H, et al. Quantitative analysis of abdominal aortic calcification in CKD patients without dialysis therapy by use of the Agatston score. Kidney Blood Press Res 2013;38:196-204.
21. Agatston AS, Janowitz WR, Hildner FJ, et al. Quantification of coronary artery calcium using ultrafast computed tomography. J Am Coll Cardiol 1990;15:827-832.
22. Kanda Y. Investigation of the freely available easy-to-use software 'EZR' for medical statistics. Bone Marrow Transplant 2013;48:452-458.
23. Okamoto T, Hatakeyama S, Kodama H, et al. The relationship between poor nutritional status and progression of aortic calcification in patients on maintenance hemodialysis. BMC Nephrol 2018;19:71.
24. Shinaberger CS, Kilpatrick RD, Regidor DL, et al. Longitudinal associations between dietary protein intake and survival in hemodialysis patients. Am J Kidney Dis 2006;48:37-49.
25. Wang J, Luo P, Yang Y, et al. Dietary protein intake and the risk of all-cause and cardiovascular mortality in maintenance hemodialysis patients: a multicenter, prospective cohort study. Nutrition 2022;95:111564.
26. Price PA, Roublick AM, Williamson MK. Artery calcification in uremic rats is increased by a low protein diet and prevented by treatment with ibandronate. Kidney Int 2006;70:1577-1583.
27. Yamada S, Tokumoto M, Tsuruya K, et al. Fetuin-A decrease induced by a low-protein diet enhances vascular calcification in uremic rats with hyperphosphatemia. Am J Physiol Renal Physiol 2015;309:F744-F754.
28. Mori K, Shoji T, Nakatani S, et al. Differential associations of fetuin-A and calcification propensity with cardiovascular events and subsequent mortality in patients undergoing hemodialysis. Clin Kidney J 2024;17:sfae042.
29. Mori K, Emoto M, Inaba M. Fetuin-A: a multifunctional protein. Recent Pat Endocr Metab Immune Drug Discov 2011;5:124-146.
30. Chen HY, Chiu YL, Hsu SP, et al. Fetuin A/nutritional status predicts cardiovascular outcomes and survival in hemodialysis patients. Am J Nephrol 2014;40:233-241.
31. Donato M, Faggin E, Cinetto F, et al. The emerging role of nutraceuticals in cardiovascular calcification: evidence from preclinical and clinical studies. Nutrients 2021;13:2603.
32. Jeon YK, Shin MJ, Saini SK, et al. Vascular dysfunction as a potential culprit of sarcopenia. Exp Gerontol 2021; 145:111220.
33. Raggi P, Cooil B, Ratti C, et al. Progression of coronary artery calcium and occurrence of myocardial infarction in patients with and without diabetes mellitus. Hypertension 2005;46:238-243.

Osaka City Med. J. Vol. 72, 49-54, 2026

Total Arch Replacement for Retrograde Aortic Dissection after Zone 2 TEVAR Employing an Axillo-axillary Bypass Graft as Arterial Perfusion

Atsutaka Aratame[1)], Masanori Sakaguchi[1)], Yosuke Sumii[1)], Ryosuke Ieguchi[1)], Shinsuke Nishimura[2)], Takeshi Ikuta[2)], and Toshio Baba[1)]

Department of Cardiovascular Surgery[1)], Bell-Land General Hospital; and Department of Cardiovascular Surgery[2)], Ishikiriseiki Hospital

Abstract

Retrograde aortic dissection is a representative one of the most serious complications from thoracic endovascular aortic repair. We report here a case of total arch replacement for retrograde aortic dissection after performing Zone2 thoracic endovascular aortic repair with left subclavian artery revascularization for a complicated Type B aortic dissection. After full heparinization following median sternotomy, the axillo-axillary bypass graft which was constructed previously for Zone2 thoracic endovascular aortic repair with left subclavian artery revascularization was resected, and the right-side graft was connected to the arterial perfusion line. The left-side bypass graft was connected to a selective cerebral perfusion line. Cardiopulmonary bypass was established via the superior and inferior venous lines and the right axillary artery. We performed total arch replacement with elephant trunk technique. The left subclavian artery perfusion was established through the new same size graft interposed between the resected previous grafts. Postoperative course was good. The patient was discharged on postoperative day 30 without any major complications. Using the axillo-axillary bypass graft as arterial perfusion lines is practical and effective to perform open repair surgery for retrograde aortic dissection after one debranching thoracic endovascular aortic repair.

Key Words: TEVAR; Total arch replacement; Retrograde aortic dissection

Introduction

In recent years, good results have been reported in cases of thoracic endovascular aortic repair (TEVAR) for complicated Type B aortic dissection (TBAD) and for uncomplicated TBAD in the acute and subacute phases[1,2)]. However, complications from TEVAR for TBAD have been increasingly reported, and retrograde aortic dissection (RTAD) is a representative one of the most serious complications. We report here a case of total arch replacement for RTAD after Zone 2 TEVAR with axillo-axillary bypass using the bypass graft as arterial perfusion.

Received July 14, 2025; accepted November 25, 2025.
Correspondence to: Atsutaka Aratame, MD.
Department of Cardiovascular Surgery, Bellland Generall Hospital,
500-3 Higasiyama, Naka-ku, Sakai city, Osaka 599-8247, Japan
Tel: +81-72-234-2001; Fax: +81-72-234-9155
E-mail: atsutaka_aratame0113@yahoo.co.jp

Case Report

A 53-year-old woman presented to our hospital with back pain. Contrast-enhanced computed tomography (CT) showed the primary entry tear was located in the lesser curvature of the distal aortic arch (Fig. 1a). She was diagnosed with TBAD and admitted for rest with antihypertensive therapy. One month later, she experienced recurrent intractable back pain, and contrast-enhanced CT revealed rapid expansion of the false lumen, although the range of dissection remained unchanged (Fig. 1b). The maximum aortic diameter was 58 mm in distal aortic arch. Due to her symptoms, rapid aortic expansion and large aortic diameter, we diagnosed complicated TBAD with an impending rupture. Zone 2 TEVAR with axillo-axillary bypass was performed to gain a healthy proximal landing zone and cover the primary entry tear. The aortic diameter of the proximal landing zone was 36 mm and the major axis diameter of the true lumen in distal landing zone was 18 mm. Firstly, a 31 mm-26 mm×10 cm tapered Conformable GORE TAG device (W. L. Gore & Associates, Flagstaff, Ariz) was deployed in the descending aorta and then, a 40 mm×15 cm Conformable GORE TAG was deployed in Zone 2. After deployment, the orifice of left subclavian artery was occluded with the 14 mm Amplatzer Vascular Plug Ⅱ (St. Jude Medical, St. Paul, MN). Postoperative contrast-enhanced CT showed thrombosis of the false lumen (Fig. 2). However, one month later, the patient suddenly complained of chest pain. Contrast-enhanced CT revealed a new tear at the proximal edge of the previous stent graft and its dislocation (Fig. 3). We planned emergency surgery. During induction of anesthesia, transesophageal echocardiography detected dissection extending from the proximal edge of the stent graft to ascending aorta (Fig. 4a). Median sternotomy was performed. After full heparinization, the previous axillo-axillary bypass graft was resected, and the right-side graft was

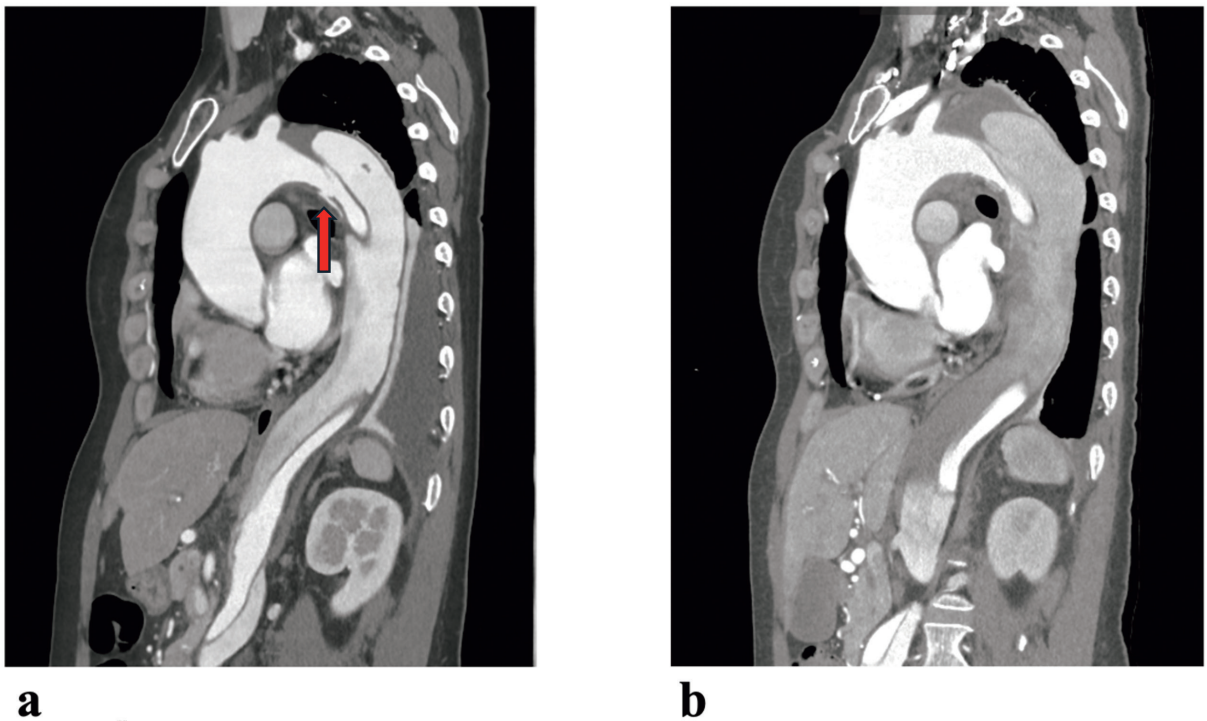

Figure 1. a, Contrast-enhanced computed tomography revealed aortic dissection extending from the left subclavian artery and the primary entry tear in the distal arch. The red arrow showed the primary entry tear.

b, Follow-up contrast-enhanced computed tomography revealed the enlargement of the false lumen one month after onset of dissection.

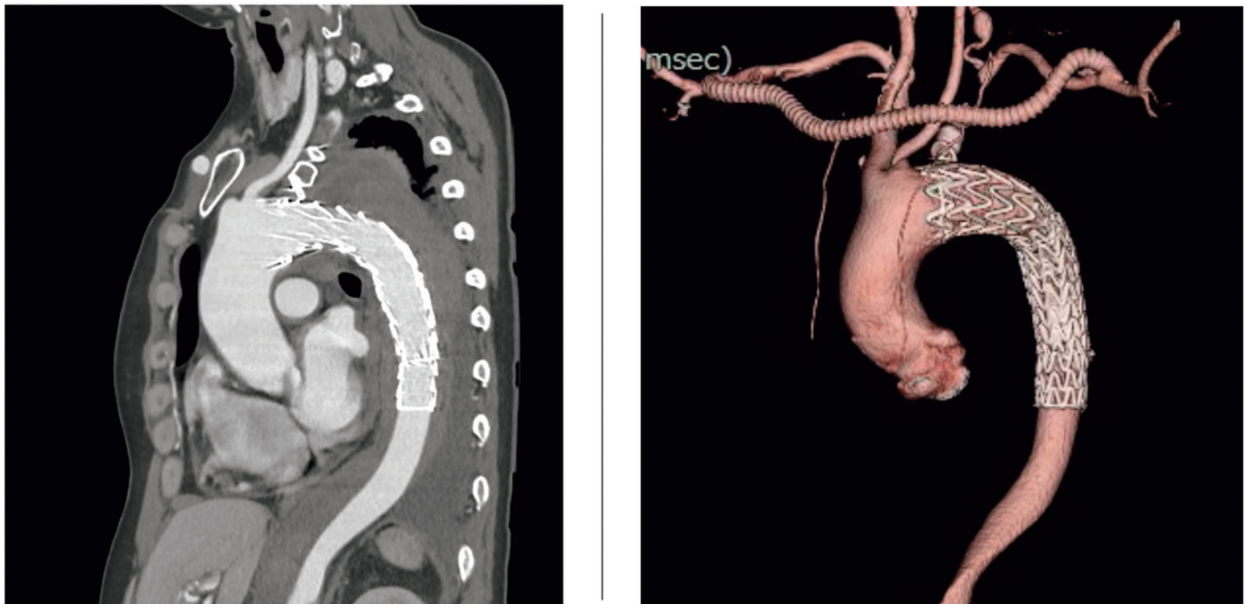

Figure 2. Postoperative contrast-enhanced computed tomography showed thrombosis of the false lumen two weeks after thoracic endovascular aortic repair.

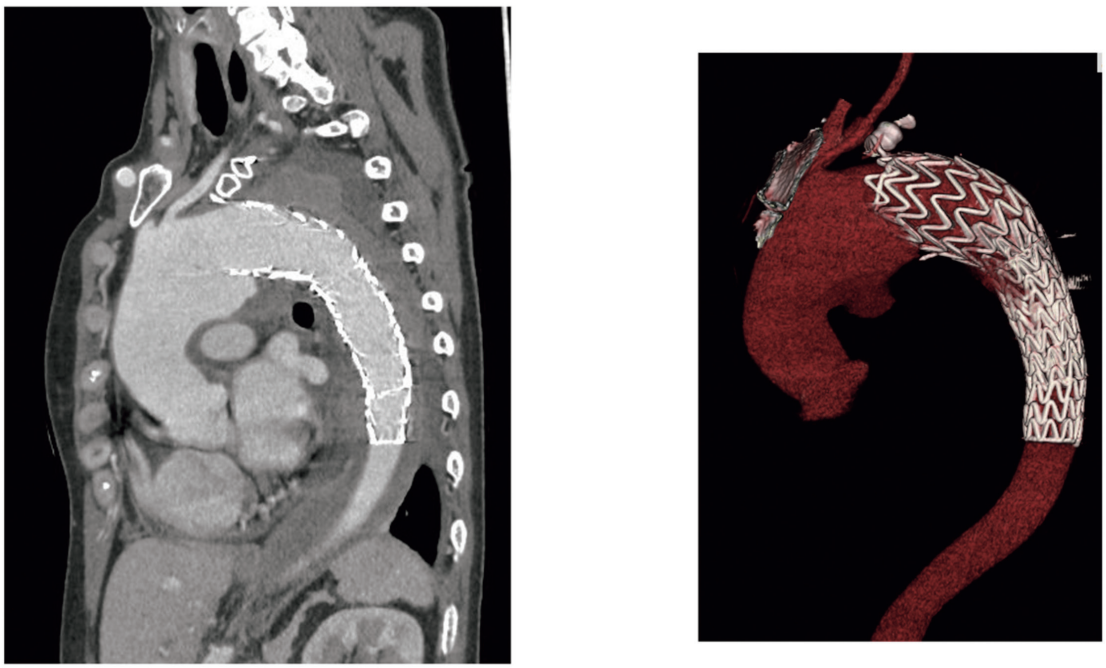

Figure 3. The proximal stent graft induced new entry and backward dislocation of the stent graft were detected.

connected to the arterial perfusion line. The left-side bypass graft was connected to a selective cerebral perfusion line. Cardiopulmonary bypass was established via the superior and inferior vena cava and the right-side graft. With careful monitoring bilateral radial arterial pressures and bilateral cerebral oxygen saturations, systemic perfusion through the right-side graft was established with a blood flow rate of 2.4 L/min/m^2 while selective cerebral perfusion through the left-side bypass graft was established with a blood flow rate of 300 mL/min. After hypothermic circulatory arrest was achieved at a rectal temperature of 26℃, the ascending aorta was resected. Intraoperative findings

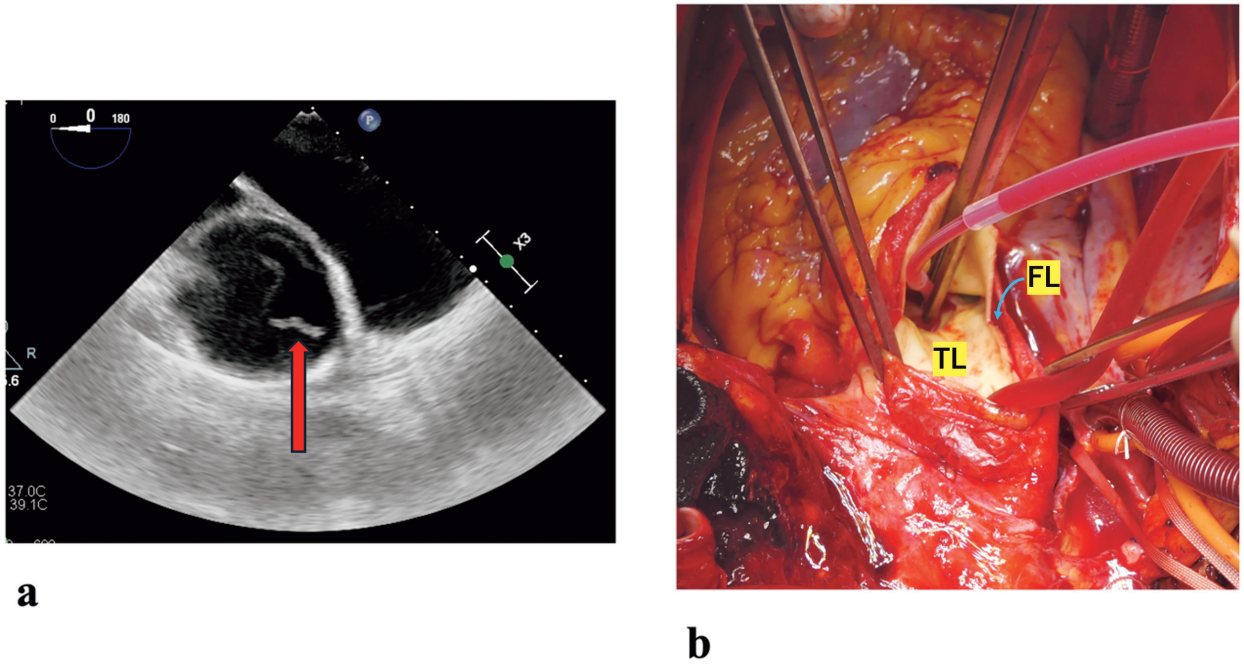

Figure 4. a, Preoperative transesophageal echocardiography detected the dissection of the ascending aorta. The red arrow showed the intimal flap.

b, Intraoperative finding revealed circumference dissection of the ascending aorta. TL denotes the true lumen, while FL denotes the false lumen.

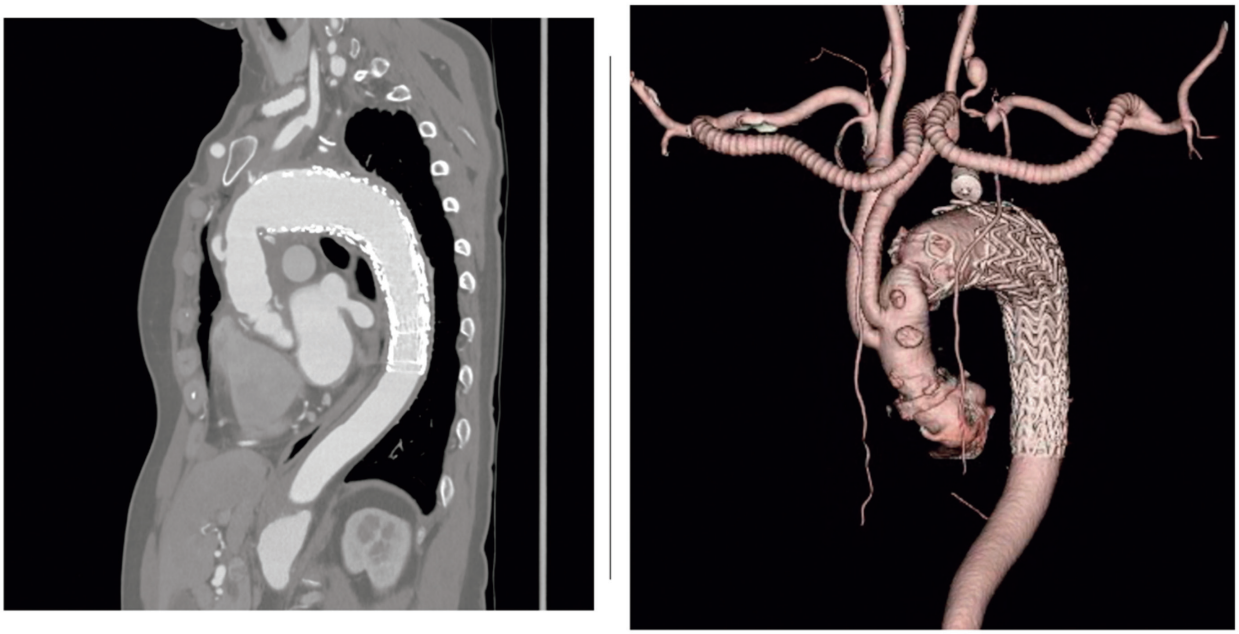

Figure 5. Contrast-enhanced computed tomography one month after total arch replacement showed the exclusion of aneurysm.

showed the circumference dissection of ascending aorta (Fig. 4b). Additional selective antegrade cerebral perfusion was gained through direct cannulation of left common carotid artery and clamping of the innominate artery. The ascending aorta was transected, and the frozen elephant trunk (39 mm 15 cm FROZENIX®J graft) was inserted into the distal aorta from Zone 0. After suturing the

proximal end of the frozen elephant trunk to the ascending aortic wall, a four-branched, 28-mm Hemashield prosthesis (Getinge, Gothenburg, Sweden) was anastomosed to the FROZENIX. After distal aortic anastomosis, proximal anastomosis was performed with double-felt-strip reinforcement with restarting systemic perfusion through the side branch of the graft. After de-clamping, the innominate and left common carotid arteries were reconstructed sequentially. The same size graft was interposed between the resected previous bypass grafts to restore a flow to left subclavian artery. Postoperative course was uneventful, and contrast-enhanced CT one month after total arch replacement showed the shrinkage of the false lumen (Fig. 5). The patient was discharged on postoperative day 30 without major complications.

Discussion

RTAD is a serious complication in TEVAR. The prevalence of RTAD has been reported to be 2.5%[3]. Although specific risk factors for RTAD are incompletely understood, pathological nature of the aorta, proximal bare stent graft, oversizing, proximal landing zone and aortic diameter may be contributing factors[3-6].

In our case, the 40 mm Conformable GORE TAG device (W. L. Gore & Associates, Flagstaff, Ariz) was deployed in a 36 mm native aorta for the complicated TBAD. We intended to avoid a large caliber change of stent grafts and mitigate radial force at the distal edge by deploying tapered stent graft in the landing zone. Oversizing ratio was about 11% in the proximal landing zone and 11.8% in the distal one. One debranching procedure was required to secure a healthy landing zone. Considering the Risk factors of RTAD, Zone 1 TEVAR with left cervical and subclavian debranching and a smaller stent graft selection might have avoided RTAD. Additionally, considering her age and operability, open surgery might have been beneficial at the point when the rapid growth of aortic false lumen was recognized.

The use of the previous bypass graft for both systemic arterial perfusion and left subclavian arterial perfusion is simple. Sueda T, et al also reported a similar case using two debranching bypass graft as a useful perfusion line[7]. Since they used the bypass graft only as selective cerebral perfusion, they needed to anastomose an additional vascular prothesis to left subclavian artery as a systemic arterial perfusion line. However, in our case, we resected the axillo-axillary bypass graft and used each cut end of the graft for systemic arterial perfusion and partial cerebral perfusion without additional vascular anastomosis. This method avoids not only time-consuming establishment of systemic arterial perfusion line but also hypertension of left subclavian artery because we can adjust circulation flow of each perfusion line. One of the drawbacks is that the interposed graft could make the bypass graft redundant. Before closing sternum, carefully positioning the graft is necessary to prevent the graft from kinking. Additionally, careful monitoring of bilateral radial arterial pressures and cerebral oxygenation is mandatory due to an irregular circulation pattern, especially in the left axillary artery.

Regarding the reconstruction of the left subclavian artery, direct anastomosis of a side branch graft to the left subclavian artery was also considered a useful option. However, this approach would require re-exposure of the anastomotic site of the left subclavian artery. In addition, the routing would need to pass through the left thoracic cavity, and we judged that such routing carried a risk of injury to the aneurysmal and dissected aortic arch. In the present case, a 40-mm stent graft had already been deployed up to Zone 2, and, as shown in Figure 3, the lesser curvature of the aortic arch

was aneurysmal. Therefore, we considered that distal anastomosis at Zone 2 was not feasible. For this reason, distal anastomosis was performed using an open stent graft from Zone 0, leaving the aneurysmal and dissected arch in situ.

Furthermore, if the aforementioned reconstruction method were employed, closure of the graft to the right subclavian artery would be required. In that case, there would be a risk of thrombus embolization from within the graft. Moreover, if complete graft explantation were undertaken, re-exposure of the anastomotic site and re-reconstruction would also be necessary, which would inevitably lead to prolongation of operative time.

As complex TEVARs have been increasing, various perfusion strategies would be necessary in unpredictable situations. In our case, separate perfusion strategy via the previous artificial vascular graft could be practical and helpful.

Acknowledgements

All authors have no COI to declare regarding the present study.

We thank English speaking editors at AJE for editing a draft of this manuscript.

References

1. Matsuda H. Treatment of uncomplicated type B aortic dissection. Gen Thorac Cardiovasc Surg 2017;65:74-79.
2. Nakajima K, Kato N, Chino S, et al. Therapeutic window for obtaining favorable remodeling after thoracic endovascular aortic repair of type B aortic dissection. J Vasc Surg 2021;75:861-867.
3. Chen Y, Zhang S, Liu L, et al. Retrograde type A aortic dissection after thoracic endovascular aortic repair: a systematic review and meta-analysis. J Am Heart Assoc 2017;6:e004649.
4. Ma T, Dong ZH, Fu WG, et al. Incidence and risk factors for retrograde type A dissection and stent graft-induced new entry after thoracic endovascular aortic repair. J Vasc Surg 2018;67:1026-1033.e2.
5. Yammine H, Briggs CS, Stanley GA, et al. Retrograde type A dissection after thoracic endovascular aortic repair for type B aortic dissection. J Vasc Surg 2019;69:24-33.
6. Canaud L, Ozdemir BA, Patterson BO, et al. Retrograde aortic dissection after thoracic endovascular aortic repair. Ann Surg 2014;260:389-395.
7. Sueda T, Takahashi S, Katayama K. Total aortic arch replacement after thoracic endovascular aortic repair using left subclavian arterial perfusion. Ann Thorac Cardiovasc Surg 2020;26:100-103.

Instructions for Authors

The Osaka City Medical Journal will consider the publication of any original manuscript, review, case report, or short communication. Articles should be in English.

Manuscript submission. Manuscripts should be sent to the Editor, Osaka City Medical Journal, Osaka City Medical Association, Graduate School of Medicine, Osaka Metropolitan University, 1-4-3 Asahimachi, Abeno-ku, Osaka 545-8585, Japan; phone and fax 06-6645-3782; e-mail gr-med-shiigakukai@omu.ac.jp

The Journal accepts only manuscripts that contain material that has not been and will not be published elsewhere. Duplicate publication of scientific data is not permitted. If closely related papers might be considered to be duplicate publications, the possible duplicate should be submitted with the manuscript and the authors should explain in their covering letter what is original in the submitted paper. Submit three copies of the manuscript (two of which may be photocopies) together with CD-R or DVD-R containing the body text, tables and figures. The manuscript should be prepared by Microsoft Word or its compatible software (doc or docx). Acceptable formats for figures are JPG or TIF. Use only 12-point font size and a standard serif font. Double-space throughout the manuscript and use standard-sized (ISO A4, 212×297 mm) white bond paper. Make margins at least 25 mm wide on all sides. Number pages consecutively starting with the title page and ending with the reference list. Begin each of these sections on a separate page: title page, abstract, text, acknowledgements, references, tables (each one separate), and figure legends. Do not use abbreviations in the title or abstract and limit their use in the text, defining each when it first appears. Manuscripts should meet the requirements outlined below to avoid delay in review and publication. Authors whose native language is not English must seek the assistance of a native English speaker who is familiar with medical sciences. Please attach the certificate from the person(s) who edit the manuscript. Some minor editorial revision of the manuscript will be made when the editorial committee considers it necessary.

Title page. All submissions must include a title page. The full title of the paper, should be concise, specific, and informative, and should contain the message of the paper without being in sentence form. Next, include the full names and academic affiliations of all authors, and indicate the corresponding author, address, phone, fax, and e-mail address. Give a running title (not to exceed 50 characters including spaces), and three to five key words. Last, give the word count for text only, exclusive of title, abstract, references, tables, and figure legends.

Structured abstract. The abstract of 250 words or less should consist of four paragraphs headed **Background, Methods, Results,** and **Conclusions.**

Text. Full papers about experiments or observations may be divided into sections headed **Introduction, Methods, Results,** and **Discussion.**

Tables. Each table should be typed on a separate sheet in characters of ordinary size, double-spaced (with at least 6 mm of white space between lines). Each table must have a title and should be assigned an Arabic numeral ('Table 3'). Vertical rules should not be used.

Figures. For black-and-white figures, submit three original glossy prints or laser-quality proofs and three photocopies of each. One transparency and three color prints should be submitted of each color figure. Label the front of figures with the figure number. Indicate on the back of each figure the first author, the first few words of the manuscript title, and the direction of the top of the figure (if needed). Photomicrographs should have scale markers that indicate the magnification. Provide figure legends on a separate page, double-spaced, immediately after the tables. All illustrations and graphs, to be referred to as figures, should be numbered in Arabic numerals ('Fig. 2' etc.). The approximate position of each figure in the text should be indicated in the right margin of the manuscript. Illustrations in full color are accepted for publication if the editors judge that color is necessary, with the cost paid by the author.

References. Reference must be double-spaced and numbered consecutively in the order cited in the text. When listing references, follow the style of the Uniform Requirements (http://www.icmje.org/) and abbreviate names of journals according to PubMed (http://www.ncbi.nlm.nih.gov/sites/netrez). List all authors up to three; when there are four or more, list the first three and use et al.

Examples of reference style

1. Priori SG, Schwartz PJ, Napolitano C, et al. Risk stratification in the long-QT syndrome. N Engl J Med 2003;348:1866-1874.
2. Schwartz PJ, Priori SG, Napolitano C. The long-QT syndrome. In: Zipes DP, Jalife J, editors. Cardiac electrophysiology: from cell to bedside. 3rd ed. Philadelphia: W.B. Saunders; 2000. pp. 597-615.

Proofs. One set of proofs together with the original manuscript will be sent to the author, to be carefully checked for any essential changes or printer's errors. The author is requested to return the corrected proofs within 48 h of their receipt.

Short communications and case reports.

1. A short communication should have between 1500 and 2000 words, including the abstract. This word count is equivalent to about four double-spaced manuscript pages.
2. The original and two copies including three sets of figures and tables should be sent to the Editorial Office.

Manuscript submission fee. A nonrefundable fee of 10,000 JPY is due on submission of original manuscripts, case reports, and short communications. A manuscript returned beyond six months of the date of the initial decision will be considered a new submission.

Page charges. A standard publication fee of 100,000 JPY will be applied for each accepted paper. Authors are also required to pay page charge of 10,000 JPY per printed page.
Ex) If your article has 10 pages, the amount of fee is 100,000 JPY+10 pages×10,000 JPY=200,000 JPY.

Reprints. If you were interested in ordering reprints of your article, we accept at least 50 full-color copies. Authors are required to pay page charge of 100 JPY per printed page. Ex) If you request 60 copies for 10-page article, the amount of fee is 100 JPY×10 pages×60 copies=60,000 JPY.

Studies of human subjects. It is the responsibility of the authors to ensure that any clinical investigation they did and report in manuscripts submitted to the Osaka City Medical Journal are in accordance with the Declaration of Helsinki (http://www.wma.net).

Animal studies. It is the responsibility of the authors to ensure that their experimental procedures are in compliance with the "Guiding Principles in the Care and Use of Animals" (http://www.the-aps.org/pub_affairs/humane/pa_aps_guiding.htm) published each month in the information for authors of the American Journal of Physiology.

Conflict of Interest (COI) Disclosure.

1. It is the responsibility of the authors to disclose any COI by signing the form.
2. If the authors have no conflicts, please state "All authors have no COI to declare regarding the present study" in the Acknowledgements.
   Authors are required to disclose any relationships with company or organization (such as funds, consultancy fee, grant, fee for speaking, stock or shares). At the time of initial submission, the corresponding author is responsible for obtaining conflict of interest information from all authors.

Theses and dissertations

Authors can include their articles, in full or in part, in a thesis or dissertation. This right allows authors to post their thesis or dissertation to their university's repository, provided that proper citation of the published article is included ([Journal Title, Year, Volume, Issue, Page numbers]).

[Revised: November 26, 2024]

COPYRIGHT TRANSFER AND STATEMENT OF ORIGINALITY

We approve the submission of this paper to the Osaka City Medical Association for publication and have taken to ensure the integrity of this work. We confirm that the manuscript is original and does not in whole or part infringe any copyright, violate any right of privacy or other personal or priority right whatever, or falsely designate the source of authorship, and that it has not been published in whole or in part and is not being submitted or considered for publication in whole or in part elsewhere (abstracts excluded).
We agree to transfer copyright the manuscript entitled

_____

_____

to the Osaka City Medical Association upon its acceptance for publication.

Write clearly and signature

(Author: print or type)	(Signature)	(Date)
_____	_____	_____
(Author: print or type)	(Signature)	(Date)
_____	_____	_____
(Author: print or type)	(Signature)	(Date)
_____	_____	_____
(Author: print or type)	(Signature)	(Date)
_____	_____	_____
(Author: print or type)	(Signature)	(Date)
_____	_____	_____
(Author: print or type)	(Signature)	(Date)
_____	_____	_____
(Author: print or type)	(Signature)	(Date)
_____	_____	_____
(Author: print or type)	(Signature)	(Date)
_____	_____	_____
(Author: print or type)	(Signature)	(Date)
_____	_____	_____

OCMJ for Conflict of Interest (COI) Disclosure Statement

The purpose of this form is to provide readers of your manuscript with information about your other interests that could influence how they receive and understand your work. The form is designed to be completed and stored electronically. Each author should submit this form and is responsible for the accuracy and completeness of the submitted information.

1. 1) Have you accepted from a sponsor or any company or organization (More than 1,000,000 JPY per year from a specific organization) ? (Please circle below)
   (1) Funds ? ····· Yes / No
   (2) Consultancy fee ? ····· Yes / No
   (3) Any grant ? ····· Yes / No
   (4) Fee for speaking ? ····· Yes / No

   2) Do you hold any stock or shares related to the manuscript ?
   (1) Directly ? ····· Yes / No
   (2) Indirectly, via family members or relatives ? ····· Yes / No

   3) If any of above items are “yes”, please provide detailed information below.

2. If none of the above apply and there is no COI please clearly state “All authors have no COI to declare regarding the present study”.

Manuscript Title:

Name / Signature_____ **Date**_____

Manuscript Identifying Number (if you know it):

The volumes and issues published in 1954-2025 were as follows: Vol 1 (one issue), Vols 2-5 (2 issues, each), Vols 6-7 (one issue, each), Vols 8-9 (2 issues, each), Vol 10 (one issue), Vol 11 (2 issues), Vol 12 (one issue), Vol 13 (2 issues), Vols 14-20 (one issue, each), Vol 21 (2 issues), Vol 22 (one issue), Vols 23-65 (2 issues, each), Vol 66 (one issue), Vol 67-71 (2 issues, each)

Publisher : Osaka City Medical Association,
Graduate School of Medicine, Osaka Metropolitan University,
1-4-3 Asahimachi, Abeno-ku, Osaka 545-8585, Japan